48. GEOPHYSICAL OBSERVATIONS COLLECTED UNDERWAY ON *GLOMAR CHALLENGER*—LEG 41

Yves Lancelot,[1] Lamont-Doherty Geological Observatory, Palisades, New York,
Eugen Seibold, Geologisch-Paläontologisches Institut der Universität, Kiel, Federal Republic of Germany,
and
James V. Gardner, Deep Sea Drilling Project, Scripps Institution of Oceanography, La Jolla, California

INTRODUCTION

Glomar Challenger departed Abidjan, Ivory Coast, on 16 February 1977 for her forty-first cruise which terminated in Malaga, Spain, on 10 April 1977. The 3344.5 nautical mile track of the ship is shown on Figure 1. Site numbers and progressive distance in hundreds of nautical miles along the track are annotated on that figure. The navigation corresponding to the track is given in Table 1. It has been acquired underway through satellite navigation system, and navigational errors are generally substantially less than 1 nautical mile (Talwani et al., 1966). Table 1 also lists the distance in nautical miles along the track and the speed and course maintained between navigation points. Also listed in Table 1 are the regional magnetic field values computed at each navigation point and used to determine the magnetic profile of Figures 2-6. Bathymetric and magnetic data on these figures have been plotted as functions of time, distance, latitude, and longitude with distance plotted as the linear function. These data have been reduced using the computer programs of Talwani (1969). The vertical scales in Figures 2-6 show magnetic values in gammas under "M" and depth in uncorrected fathoms under "D." The bathymetric profile appears as a thin line in the upper part of the figures and the magnetic profile is the darker line in the lower part. At the top of the figures from top to bottom are annotated time in days, time in hours, latitude in degrees, and longitude in degrees. Along the bottom all navigation points are marked and occasionally annotated along with the course and speed that were subsequently maintained. On the bottommost scale is the distance along the track in nautical miles. The site locations have also been indicated directly on the bathymetric profiles.

The second series of figures (Figures 7-39) shows the seismic reflection records (as a linear function of time). Depth in reflection times (seconds) is indicated on the side of the profiles. At the bottom of the profiles we also added indication of time in days and hours, and speed and heading maintained. Distances along the ship track, in hundreds of nautical miles, and site locations are annotated at the top of the profiles. The sound source used for obtaining these records consisted generally of two airguns with 10- and 40-in³ capacities. Profiles were recorded on dry paper EDO recorders set on a 10-second sweep rate.

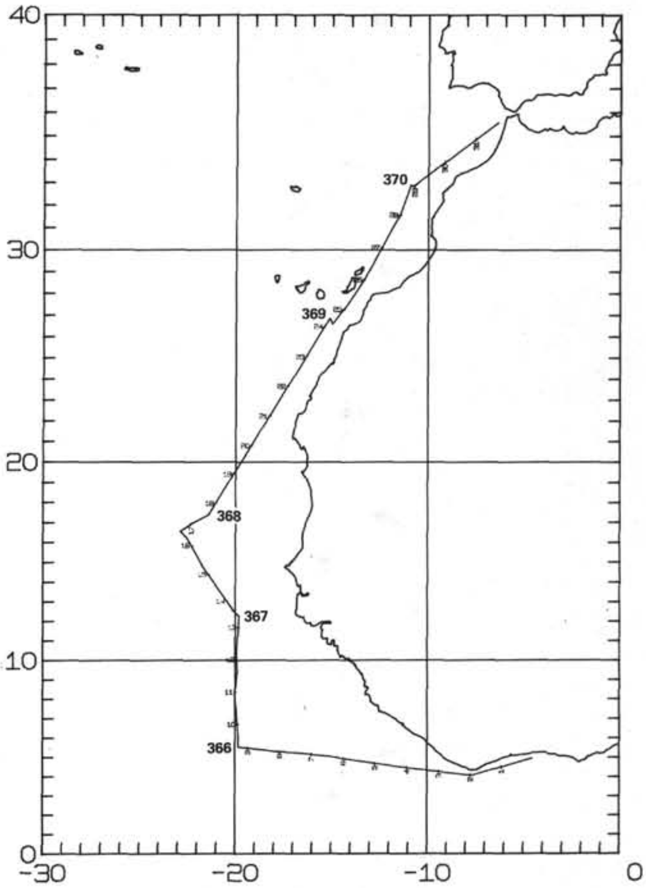

Figure 1. *Track chart for Leg 41 of* Glomar Challenger *from Abidjan, Ivory Coast, to Malaga, Spain. Small numbers are distance along the track in hundreds of nautical miles.*

MAGNETICS

Most of the track of *Glomar Challenger* during this cruise stays within the Jurassic Quiet Zone except in the vicinity of Sites 367 (Cape Verde Basin) and 368 (Cape Verde Rise). Therefore the magnetic profiles of Figures 2-6 are of limited interest as far as the identification of

[1]Present address: Laboratoire de Géologie Dynamique, Université Pierre et Marie Curie, Paris, France.

TABLE 1
List of Navigation Points for Underway Portion of Leg 41 of the *Glomar Challenger*[a]

	Time (GMT)	Latitude (N)	Longitude (W)	Distance (nautical miles)	Speed (knots)	Course	Regional Magnetic Field (gammas)
February							
18	406	4°57.9′	4°57.9′	0.0	8.1	255	30969.
18	600	4°54.0′	4°47.7′	15.4	8.1	253	30933.
18	744	4°49.8′	5°01.2′	29.5	8.5	251	30899.
18	930	4°45.0′	5°15.5′	44.6	8.7	254	30862.
18	1046	4°42.0′	5°26.2′	55.7	8.7	253	30836.
18	1134	4°40.0′	5°32.9′	62.6	8.8	253	30819.
18	1322	4°35.3′	5°48.1′	78.5	8.8	254	30781.
18	1356	4°33.9′	5°52.9′	83.5	9.0	254	30769.
18	1834	4°22.3′	6°32.9′	125.0	9.4	253	30670.
18	2010	4°18.0′	6°47.4′	140.1	9.5	270	30635.
18	2022	4°18.0′	6°49.3′	142.0	9.7	270	30631.
18	2035	4°18.0′	6°51.4′	144.1	9.6	255	30627.
19	000	4°09.3′	7°23.0′	176.8	9.5	254	30551.
19	054	4°07.0′	7°31.3′	185.4	9.6	253	30531.
19	128	4°05.4′	7°36.5′	190.8	9.7	251	30518.
19	147	4°04.4′	7°39.4′	193.8	9.5	275	30510.
19	310	4°05.5′	7°52.5′	207.0	9.5	276	30490.
19	458	4°07.4′	8°09.6′	224.1	9.4	273	30463.
19	530	4°07.7′	8°14.6′	229.1	9.6	274	30455.
19	550	4°07.9′	8°17.8′	232.3	9.1	297	30450.
19	612	4°09.4′	8°20.8′	235.7	8.9	297	30448.
19	615	4°09.6′	8°21.2′	236.1	9.0	274	30448.
19	758	4°10.8′	8°36.7′	251.6	8.2	275	30423.
19	840	4°11.3′	8°42.4′	257.3	9.3	274	30415.
19	940	4°11.9′	8°51.7′	266.6	8.7	274	30400.
19	1028	4°12.4′	8°58.7′	273.6	9.2	277	30389.
19	1126	4°13.5′	9°07.5′	282.5	9.2	277	30376.
19	1230	4°14.7′	9°17.3′	292.3	9.0	270	30362.
19	1232	4°14.7′	9°17.6′	292.6	8.5	278	30361.
19	1306	4°15.4′	9°22.4′	297.4	8.7	279	30355.
19	1446	4°17.7′	9°36.7′	311.9	8.7	278	30336.
19	1632	4°19.8′	9°52.0′	327.3	8.6	277	30315.
19	1934	4°23.0′	10°17.9′	353.3	9.0	275	30279.
19	2014	4°23.5′	10°23.9′	359.3	8.2	276	30271.
19	2112	4°24.3′	10°31.8′	367.2	8.8	275	30260.
19	2202	4°25.0′	10°39.1′	374.5	9.0	275	30249.
19	2256	4°25.7′	10°47.2′	382.6	8.8	277	30238.
20	000	4°26.8′	10°56.6′	392.1	9.1	279	30225.
20	004	4°26.9′	10°57.2′	392.7	9.2	278	30224.
20	038	4°27.6′	11°02.4′	397.9	9.0	277	30218.
20	402	4°31.3′	11°32.8′	428.5	9.1	277	30178.
20	710	4°34.8′	12°01.1′	456.9	9.3	278	30143.
20	754	4°35.8′	12°07.9′	463.7	8.8	278	30135.
20	938	4°37.8′	12°23.1′	479.0	9.0	277	30117.
20	1018	4°38.5′	12°29.1′	485.0	9.3	277	30109.
20	1222	4°41.0′	12°48.3′	504.3	8.9	339	30087.
20	1235	4°42.8′	12°49.0′	506.3	9.3	277	30091.
20	1536	4°46.4′	13°17.0′	534.4	9.3	279	30059.
20	1844	4°51.1′	13°45.8′	563.5	9.2	278	30031.
20	2032	4°53.4′	14°02.2′	580.0	9.5	278	30014.
20	2150	4°55.1′	14°14.5′	592.4	9.5	279	30002.
21	000	4°58.2′	14°35.0′	613.0	9.5	279	29983.
21	132	5°00.4′	14°49.5′	627.6	9.5	279	29970.
21	205	5°01.2′	14°54.7′	632.9	9.6	277	29966.
21	308	5°02.4′	15°04.8′	643.0	9.6	276	29956.
21	454	5°04.3′	15°21.7′	659.9	9.6	275	29939.
21	624	5°05.6′	15°36.1′	674.3	9.7	276	29925.
21	808	5°07.4′	15°52.8′	691.1	9.5	278	29909.
21	1038	5°10.6′	16°16.5′	714.9	10.0	279	29809.
21	1058	5°11.1′	16°19.8′	718.2	9.4	279	29888.
21	1310	5°14.4′	16°40.2′	738.8	9.1	279	29875.

[a]Also tabulated are distance along track, courses and speeds maintained between navigation points, and regional magnetic field values.

TABLE 1 – *Continued*

	Time (GMT)	Latitude (N)	Longitude (W)	Distance (nautical miles)	Speed (knots)	Course	Regional Magnetic Field (gammas)
February–*Continued*							
21	1345	5°15.2′	16°45.5′	744.1	9.1	272	29871.
21	1448	5°15.5′	16°55.1′	753.7	9.0	272	29861.
21	1628	5°16.1′	17°10.2′	768.7	9.0	272	29846.
21	2022	5°17.3′	17°45.6′	804.0	9.0	273	29810.
21	2100	5°17.6′	17°51.3′	809.7	8.9	278	29805.
21	2210	5°19.1′	18°01.6′	820.1	8.8	276	29800.
22	000	5°20.9′	18°17.7′	836.2	8.8	277	29789.
22	202	5°23.0′	18°35.6′	854.1	8.7	279	29779.
22	358	5°52.3′	18°52.3′	871.0	8.6	277	29772.
22	720	5°28.9′	19°21.3′	900.0	8.7	278	29757.
22	800	5°29.7′	19°27.1′	905.9	8.7	274	29755.
22	908	5°30.4′	19°37.0′	915.7	8.7	276	29749.
22	946	5°31.0′	19°42.5′	921.2	9.3	272	29747.
22	1036	5°31.3′	19°50.3′	929.0	9.7	4	29741.
22	1109	5°36.6′	19°49.9′	934.3	9.6	343	29762.
22	1130	5°39.8′	19°50.9′	937.7	5.5	348	29773.
22	1140	5°40.7′	19°51.1′	938.6	0.0	90	29777.
March							
1	1702	5°40.7′	19°51.1′	938.6	5.0	334	29776.
1	1710	5°41.3′	19°51.4′	939.3	8.5	357	29778.
1	1836	5°53.4′	19°52.0′	951.4	8.9	358	29825.
1	2022	6°09.1′	19°52.6′	967.1	9.2	358	29887.
1	2056	6°14.3′	19°52.8′	972.3	8.8	359	29907.
1	2304	6°33.1′	19°53.0′	991.1	8.9	356	29983.
2	000	6°41.4′	19°53.6′	999.4	8.9	356	30017.
2	050	6°48.8′	19°54.1′	1006.8	8.9	356	30047.
2	240	7°05.0′	19°55.3′	1023.1	8.4	357	30115.
2	614	7°34.8′	19°56.8′	1052.9	8.5	353	30243.
2	700	7°41.3′	19°57.6′	1059.5	8.4	355	30271.
2	800	7°49.7′	19°58.3′	1067.9	8.5	356	30308.
2	834	7°54.5′	19°58.6′	1072.7	8.6	357	30329.
2	944	8°04.5′	19°59.1′	1082.7	8.9	356	30374.
2	1024	8°10.4′	19°59.5′	1088.6	9.0	355	30401.
2	1100	8°15.8′	20°00.0′	1094.0	8.8	1	30425.
2	1128	8°19.9′	19°59.9′	1098.2	8.7	3	30444.
2	1230	8°28.9′	19°59.5′	1107.2	8.9	5	30486.
2	1420	8°45.1′	19°58.0′	1123.4	8.7	4	30563.
2	1520	8°53.8′	19°57.4′	1132.1	8.8	6	30605.
2	1814	9°54.9′	19°54.9′	1157.8	5.6	4	30729.
2	1829	9°20.7′	19°54.8′	1159.2	9.0	6	30736.
2	1835	9°21.6′	19°54.7′	1160.1	8.8	0	30740.
2	1932	9°30.0′	19°54.7′	1168.5	9.0	1	30782.
2	2008	9°35.4′	19°54.6′	1173.9	9.3	357	30809.
2	2116	9°45.9′	19°55.2′	1184.4	9.3	358	30861.
2	2300	10°02.0′	19°55.7′	1200.5	9.2	358	30942.
3	000	10°11.2′	19°56.0′	1209.7	9.3	358	30989.
3	246	10°36.8′	19°56.8′	1235.3	9.0	359	31123.
3	320	10°41.9′	19°56.9′	1240.4	9.1	6	31150.
3	432	10°52.7′	19°55.7′	1251.7	8.8	6	31207.
3	748	11°21.2′	19°52.4′	1280.0	9.0	6	31362.
3	825	11°26.7′	19°51.8′	1285.5	8.9	1	31393.
3	934	11°36.9′	19°51.6′	1295.7	8.7	2	31449.
3	1052	11°48.2′	19°51.1′	1307.0	7.5	0	31513.
3	1100	11°49.2′	19°51.1′	1308.0	8.7	3	31518.
3	1142	11°55.3′	19°50.8′	1314.1	8.8	3	31553.
3	1415	12°17.6′	19°49.6′	1336.4	8.8	308	31680.
3	1426	12°18.6′	19°50.9′	1338.1	9.4	309	31686.
3	1430	12°19.0′	19°51.4′	1338.7	7.1	309	31688.
3	1545	12°24.6′	19°58.5′	1347.6	7.1	313	31720.

TABLE 1 – *Continued*

	Time (GMT)	Latitude (N)	Longitude (W)	Distance (nautical miles)	Speed (knots)	Course	Regional Magnetic Field (gammas)
March–*Continued*							
3	1612	12°26.8′	20°00.9′	1350.8	6.9	318	31733.
3	1640	12°29.2′	20°03.1′	1354.0	5.0	319	31747.
3	1707	12°30.9′	20°04.6′	1356.3	9.3	141	31757.
3	1712	12°30.3′	20°04.1′	1357.1	8.4	131	31753.
3	1724	12°29.2′	20°02.8′	1358.7	0.0	136	31747.
11	317	12°29.1′	20°02.7′	1358.9	8.4	316	31746.
11	318	12°29.2′	20°02.8′	1359.0	6.2	307	31746.
11	350	12°31.2′	20°05.5′	1362.3	5.7	327	31758.
11	405	12°32.4′	20°06.3′	1363.8	8.5	324	31765.
11	418	12°33.9′	20°07.4′	1365.6	8.7	325	31774.
11	606	12°46.8′	20°16.6′	1381.3	8.6	326	31851.
11	754	12°59.6′	20°25.5′	1396.8	8.6	326	31928.
11	1034	13°18.6′	20°38.6′	1419.7	8.5	325	32045.
11	1736	14°07.1′	21°14.2′	1479.2	8.5	323	32359.
11	1800	14°09.8′	21°16.3′	1482.6	8.3	326	32377.
11	1948	14°22.2′	21°25.0′	1497.6	8.3	326	32460.
11	2134	14°34.4′	21°33.4′	1512.3	8.5	327	32543.
12	000	14°51.7′	21°45.1′	1532.9	8.6	327	32663.
12	015	14°53.5′	21°46.3′	1535.1	8.4	333	32675.
12	704	15°44.6′	22°13.7′	1592.6	8.4	335	33038.
12	730	15°47.9′	22°15.3′	1596.3	8.7	330	33062.
12	734	15°48.4′	22°15.6′	1596.8	8.5	330	33066.
12	906	15°59.7′	22°22.4′	1609.9	8.9	328	33149.
12	1050	16°12.7′	22°30.9′	1625.2	8.9	328	33247
12	1130	16°17.7′	22°34.2′	1631.2	8.3	316	33284.
12	1131	16°17.8′	22°34.3′	1631.3	9.0	309	33285.
12	1252	16°25.4′	22°44.2′	1643.5	10.6	314	33347.
12	1335	16°30.7′	22°49.9′	1651.1	6.6	316	33389.
12	1430	16°35.0′	22°54.3′	1657.1	0.0	90	33424.
12	1740	16°35.0′	22°54.3′	1657.1	10.5	169	33424.
12	1754	16°32.6′	22°53.8′	1659.5	7.7	56	33406.
12	1830	16°35.2′	22°49.8′	1664.2	3.7	62	33421.
12	1837	16°35.4′	22°49.4′	1664.6	7.7	56	33422.
12	2044	16°44.5′	22°35.2′	1681.0	7.8	52	33476.
12	2256	16°55.1′	22°21.1′	1698.1	7.9	52	33542.
12	2332	16°58.0′	22°17.2′	1702.9	7.9	62	33560.
13	000	16°59.7′	22°13.8′	1706.5	7.6	61	33569.
13	018	17°00.8′	22°11.7′	1708.8	8.1	61	33576.
13	044	17°02.5′	22°08.5′	1712.3	8.0	63	33586.
13	204	17°07.3′	21°58.6′	1722.9	8.1	64	33613.
13	226	17°08.6′	21°55.8′	1725.9	8.0	64	33620.
13	412	17°14.9′	21°42.5′	1740.1	8.1	66	33656.
13	500	17°17.5′	21°36.3′	1746.6	8.0	61	33671.
13	616	17°22.4′	21°27.0′	1756.7	7.9	68	33700.
13	630	17°23.1′	21°25.2′	1758.6	7.6	28	33704.
13	735	17°30.4′	21°21.2′	1766.8	0.0	90	33754.
20	1107	17°30.4′	21°21.2′	1766.8	8.2	32	33754.
20	1724	18°14.3′	20°52.9′	1818.3	8.0	32	34057.
20	1912	18°26.6′	20°44.9′	1832.7	7.8	32	34143.
20	1930	18°28.6′	20°43.6′	1835.1	8.1	30	34157.
20	2034	18°36.1′	20°39.0′	1843.8	8.2	32	34209.
20	2118	18°41.2′	20°35.7′	1849.8	8.0	32	34245.
20	2148	18°44.6′	20°33.5′	1853.7	7.9	31	34269.
20	2220	18°48.2′	20°31.2′	1858.0	8.1	33	34295.
20	2332	18°56.4′	20°25.6′	1867.7	8.1	30	34353.
21	000	18°59.7′	20°23.6′	1871.5	8.1	30	34376.
21	210	19°14.9′	20°14.4′	1889.0	8.0	29	34485.
21	356	19°27.3′	20°07.1′	1903.2	8.3	33	34574.
21	510	19°35.9′	20°01.1′	1913.5	8.2	32	34636.
21	656	19°48.1′	19°52.9′	1927.9	8.4	36	34724.
21	718	19°50.6′	19°51.0′	1931.0	8.1	34	34742.
21	752	19°54.4′	19°54.4′	1935.6	8.3	34	34769.
21	906	20°02.9′	19°42.2′	1945.8	8.0	34	34830.
21	936	20°06.2′	19°39.8′	1949.8	8.0	33	34854.

TABLE 1 – *Continued*

	Time (GMT)	Latitude (N)	Longitude (W)	Distance (nautical miles)	Speed (knots)	Course	Regional Magnetic Field (gammas)
March–*Continued*							
21	1120	20°17.9′	19°31.7′	1963.8	7.9	32	34939.
21	1354	20°35.1′	19°20.3′	1984.0	8.0	32	35066.
21	1542	20°47.3′	19°12.2′	1998.4	8.0	30	35156.
21	1636	20°53.5′	19°08.3′	2005.6	8.0	32	35202.
21	1820	21°05.2′	19°00.5′	2019.4	8.0	31	35289.
21	2028	21°19.9′	18°51.0′	1036.5	7.6	31	35398.
21	1338	21°40.6′	18°37.8′	2060.6	7.6	30	35554.
22	000	21°43.0′	18°36.3′	2063.4	7.6	31	35572.
22	114	21°51.0′	18°31.1′	2072.7	8.0	31	35633.
22	300	22°03.1′	18°23.2′	2086.9	8.4	32	35724.
22	424	22°13.1′	18°16.4′	2098.7	8.3	34	35800.
22	608	22°25.1′	18°07.7′	2113.1	7.8	29	35891.
22	630	22°27.6′	18°06.2′	2116.0	8.0	30	35911.
22	816	22°39.9′	17°58.5′	2130.2	7.9	31	36005.
22	1014	22°53.2′	17°49.7′	2145.8	7.9	29	36107.
22	1034	22°55.5′	17°48.3′	2148.4	8.2	32	36125.
22	1126	23°01.5′	17°44.2′	2155.5	8.3	33	36171.
22	1302	23°12.6′	17°36.3′	21€8.8	8.3	28	36257.
22	1446	23°25.3′	17°28.8′	2183.2	8.2	31	36356.
22	2008	24°03.1′	17°03.7′	2227.4	8.7	31	36651.
22	2150	24°15.7′	16°55.3′	2242.2	9.5	332	36749.
22	2155	24°16.4′	16°55.7′	2243.0	8.7	31	36755.
22	2248	24°23.0′	16°51.3′	2250.7	8.1	31	36807.
22	2340	24°29.0′	16°47.3′	2257.7	8.4	31	36854.
23	000	24°31.4′	16°45.7′	2260.5	8.3	33	36873.
23	036	24°35.6′	16°42.7′	2265.5	8.2	34	36906.
23	520	25°07.6′	16°18.9′	2304.3	8.3	33	37161.
23	555	25°11.9′	16°16.0′	2309.2	8.7	14	37193.
23	600	25°12.6′	16°15.8′	2309.9	8.5	17	37199.
23	620	25°15.3′	16°14.9′	2312.7	8.4	33	37220.
23	906	25°34.9′	16°00.9′	2336.0	8.2	33	37376.
23	933	25°38.0′	15°58.7′	2339.7	5.3	34	37401.
23	944	25°38.8′	15°58.1′	2340.7	8.2	29	37407.
23	1132	25°51.8′	15°50.2′	2355.5	8.5	32	37512.
23	1226	25°58.3′	15°45.7′	2363.2	8.5	35	37563.
23	1352	26°08.3′	15°38.0′	1375.3	7.9	33	37643.
23	1610	26°23.6′	15°27.1′	2393.5	7.9	26	37766.
23	1642	26°27.4′	15°25.0′	2397.7	7.1	32	37797.
23	1655	26°28.7′	15°24.1′	2399.3	3.7	17	37807.
23	1700	26°29.0′	15°24.0′	2399.6	7.2	30	37809.
23	1850	26°40.4′	15°16.7′	2412.7	7.1	28	37901.
23	2034	26°51.3′	15°10.3′	2425.0	9.7	22	37989.
23	2040	26°52.2′	15°09.9′	2426.0	9.0	153	37997.
23	2235	26°36.9′	15°01.1′	2443.2	5.3	157	37868.
23	2256	26°35.2′	15°00.3′	2445.0	6.4	146	37854.
23	2314	26°33.6′	14°59.1′	2446.9	6.1	340	37841.
23	2335	26°35.6′	14°59.9′	2449.1	0.0	90	37857.
26	2225	26°35.6′	14°59.9′	2449.1	5.0	37	37857.
26	2246	26°37.0′	14°58.7′	2450.8	8.2	38	37868.
27	000	26°45.0′	14°51.8′	2460.9	8.3	37	37933.
27	040	26°49.4′	14°48.1′	2466.4	8.4	38	37968.
27	400	27°11.5′	14°29.0′	2494.3	8.5	39	38146.
27	043	27°14.8′	14°26.0′	2498.6	8.6	36	38172.
27	542	27°23.2′	14°19.2′	2508.9	8.3	33	38240.
27	602	27°25.5′	14°17.5′	2511.7	8.6	35	38259.
27	746	27°37.7′	14°07.8′	2526.6	8.9	35	38357.
27	810	27°40.6′	14°05.5′	2530.1	8.9	35	38381.
27	956	27°53.6′	13°55.4′	2545.9	8.9	34	38486.
27	1044	27°59.5′	13°50.9′	2553.0	9.2	34	38534.
27	1230	28°12.9′	13°40.5′	2569.3	8.7	34	38643.
27	1530	28°34.5′	13°23.8′	2595.4	8.7	26	38818.
27	1720	28°48.8′	13°15.8′	2611.3	8.7	28	38934.
27	1906	29°02.3′	13°07.6′	2626.6	8.7	26	39044.
27	1935	29°06.1′	13°05.5′	2630.8	8.4	28	39075.

TABLE 1 – *Continued*

	Time (GMT)	Latitude (N)	Longitude (W)	Distance (nautical miles)	Speed (knots)	Course	Regional Magnetic Field (gammas)
March–*Continued*							
27	1952	29°08.2′	13°04.2′	2633,2	9.2	29	39092.
27	2122	29°20.2′	12°56.5′	2647.0	9.3	28	39190.
27	2202	29°25.7′	12°53.2′	2653.2	9.1	27	39235.
27	2308	29°34.6′	12°47.9′	2663.2	9.6	30	39307.
27	2348	29°40.1′	12°44.2′	2669.6	9.5	33	39352.
28	000	29°41.7′	12°43.0′	2671.5	9.4	33	39365.
28	100	29°49.6′	12°37.2′	2680.8	9.5	30	39429.
28	246	30°04.2′	12°27.6′	2697.6	9.7	30	39547.
28	514	30°25.1′	12°13.9′	2721.7	9.8	30	39717.
28	545	30°29.5′	12°11.0′	2726.7	9.8	28	39752.
28	544	30°38.0′	12°05.7′	2736.4	9.8	28	39821.
28	846	30°55.6′	11°55.0′	2756.2	9.9	28	39964.
28	916	31°00.0′	11°52.3′	2761.2	10.0	29	39999.
28	956	31°05.8′	11°48.5′	2767.9	10.0	28	40046.
28	1102	31°15.5′	11°42.5′	2778.8	10.1	29	40124.
28	1250	31°31.4′	11°32.0′	2797.1	10.1	20	40252.
28	1438	31°48.5′	11°24.8′	2815.2	9.6	19	40390.
28	1612	32°02.7′	11°19.2′	2830.2	9.5	20	40503.
28	1758	32°18.5′	11°12.5′	2847.0	9.5	19	40630.
28	1818	32°21.5′	11°11.3′	2850.2	9.4	24	40654.
28	1848	32°25.8′	11°09.0′	2854.9	9.1	22	40688.
28	2000	32°36.0′	11°04.2′	2865.9	8.8	21	40769.
28	2032	32°40.4′	11°02.2′	2870.6	9.5	19	40804.
28	2151	32°52.2′	10°57.5′	2883.0	10.1	106	40898.
28	2202	32°51.7′	10°55.4′	2884.9	6.7	110	40894.
28	2218	32°51.1′	10°53.4′	2886.6	7.6	101	40889.
28	2247	32°50.4′	10°49.1′	2890.3	4.6	98	40883.
28	2307	32°50.2′	10°47.3′	2891.8	7.5	100	40882.
28	2335	32°49.6′	10°43.2′	2895.3	5.6	285	40877.
29	000	32°50.2′	10°45.9′	2897.7	6.0	280	40882.
29	006	32°50.3′	10°46.6′	2898.3	0.0	90	40883.
April							
8	157	32°50.3′	10°46.6′	2898.3	4.9	49	40883.
8	212	32°51.1′	10°45.5′	2899.5	7.1	50	40889.
8	310	32°55.5′	10°39.2′	2906.4	7.6	50	40924.
8	456	33°04.2′	10°27.0′	2919.8	7.3	48	40993.
8	650	33°13.4′	10°14.6′	2933.7	7.4	52	41066.
8	715	33°15.3′	10°11.7′	2936.8	7.4	53	41081.
8	850	33°22.3′	10°00.5′	2948.5	7.6	52	41137.
8	1138	33°35.3′	9°40.2′	2969.8	7.7	53	41240.
8	1324	33°43.6′	9°27.2′	2983.4	7.7	53	41306.
8	1850	34°08.8′	8°46.8′	3025.4	8.0	53	41506.
8	2028	34°16.6′	8°34.2′	3038.4	7.9	54	41568.
8	2216	34°24.9′	8°20.2′	3052.6	7.6	54	41634.
9	000	34°32.7′	8°07.3′	3065.8	7.6	54	41696.
9	408	34°51.2′	7°36.5′	3097.2	7.6	55	41843.
9	558	34°59.1′	7°22.5′	3111.1	7.6	54	41906.
9	824	35°10.0′	7°04.2′	3129.6	7.5	54	41993.
9	1012	35°17.9′	6°50.8′	3143.1	7.4	51	42056.
9	1046	35°20.5′	6°46.8′	3147.3	8.0	54	42076.
9	1330	35°33.4′	6°25.2′	3169.1			42179.

anomalies of the sea-floor spreading type are concerned. Most of the variations observed are related directly to volcanic piles such as Sierra Leone Rise, Cape Verde Islands and associated seamounts, and Canary Islands. The only areas where magnetic lineations have been crossed, although very obliquely, are the Cape Verde Basin, shortly after leaving Site 367 and before reaching the Cape Verde Islands, and the Cape Verde Basin, between the Cape Verde Islands and Site 368. The Quiet Zone Boundary can be clearly identified near Site 368, approximately at the top of the Cape Verde Rise (at 1600 hr 20 April 1975 on the profile). It can also tentatively be identified near Site 367 at a point around 1100 on 11 April 1975. In both cases it corresponds very well with the boundary identified by Hayes and Rabinowitz (1975). Some Mesozoic anomalies on the seaward side of the Quiet Zone Boundary are visible on the profiles, but the ship track cut through them so obliquely that no attempt was made at identifying them.

GL-41

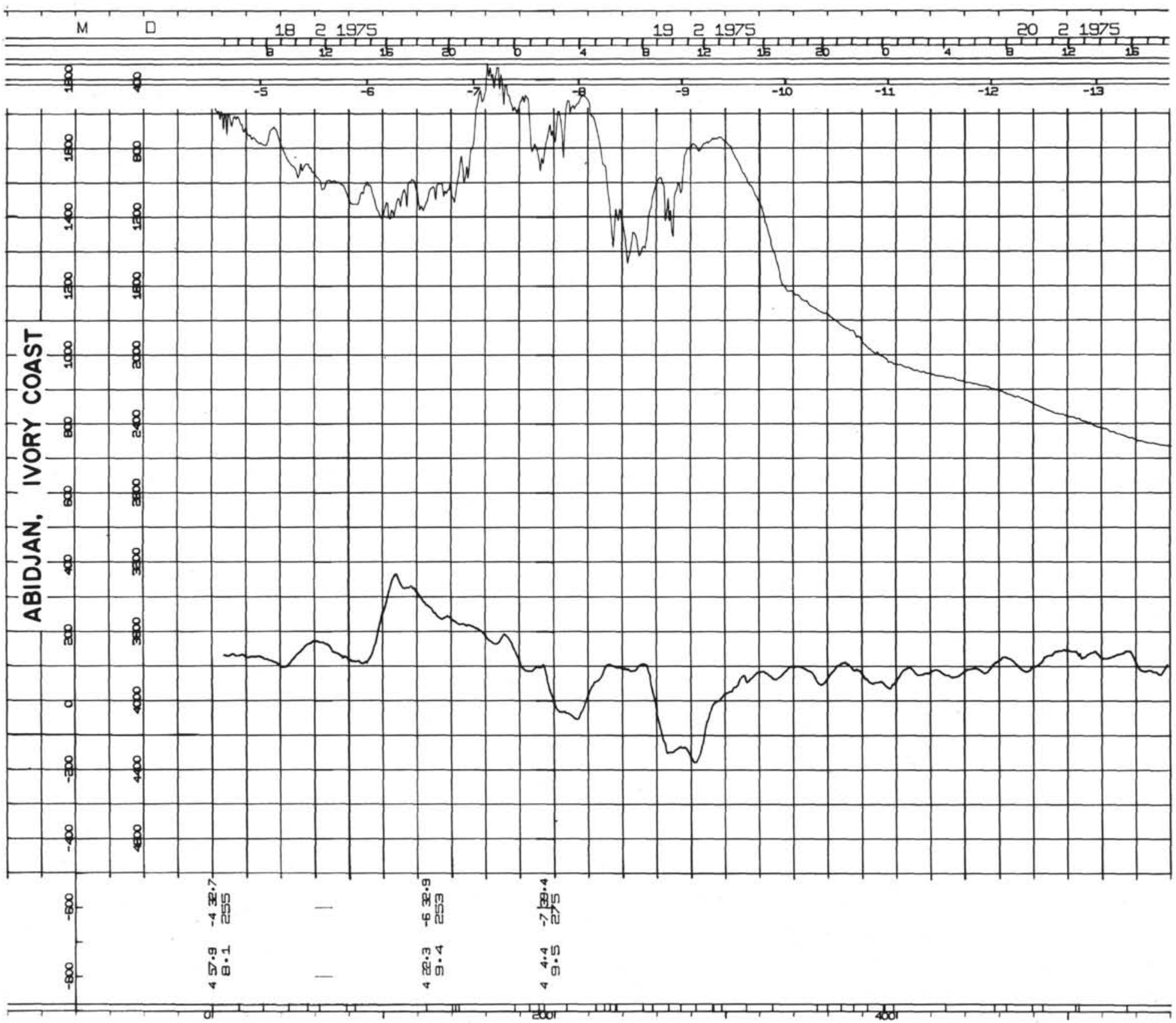

Figure 2. *Bathymetric and magnetic profiles along the track of Leg 41 of* Glomar Challenger. *Plots and scales explained in text.*

GL-41

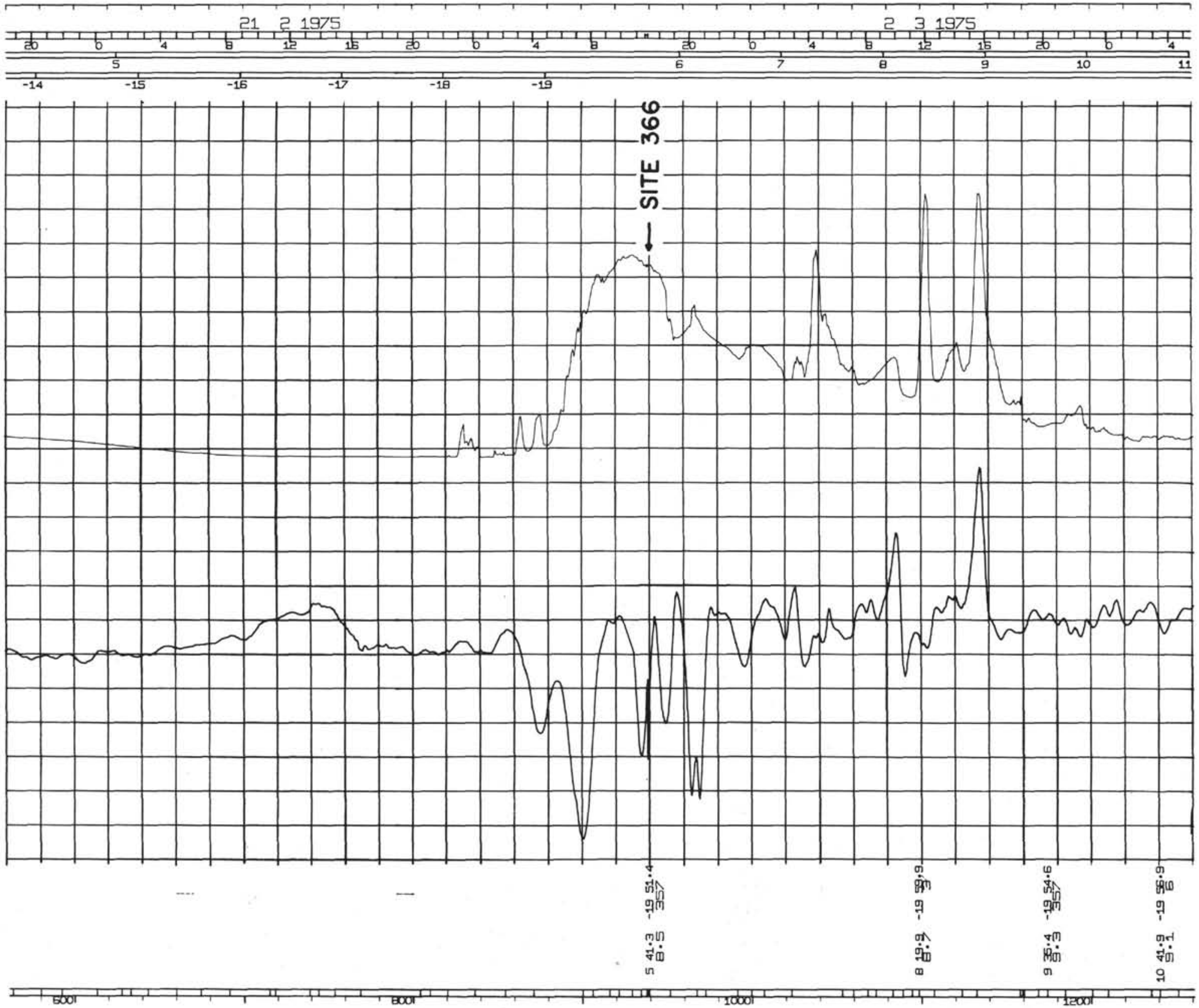

Figure 3. *Bathymetric and magnetic profiles along the track of Leg 41 of* Glomar Challenger. *Plots and scales explained in text.*

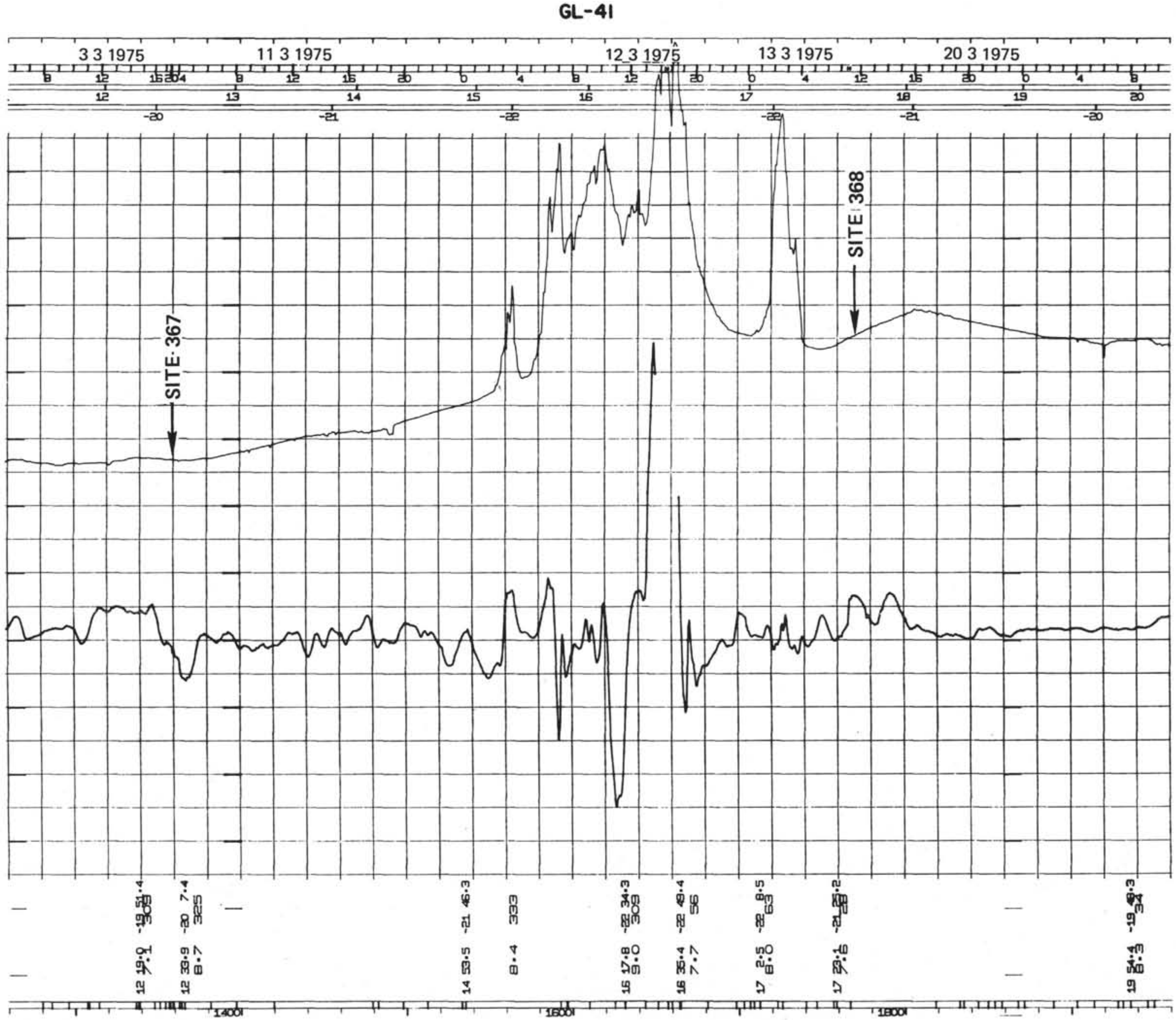

Figure 4. *Bathymetric and magnetic profiles along the track of Leg 41 of* Glomar Challenger. *Plots and scales explained in text.*

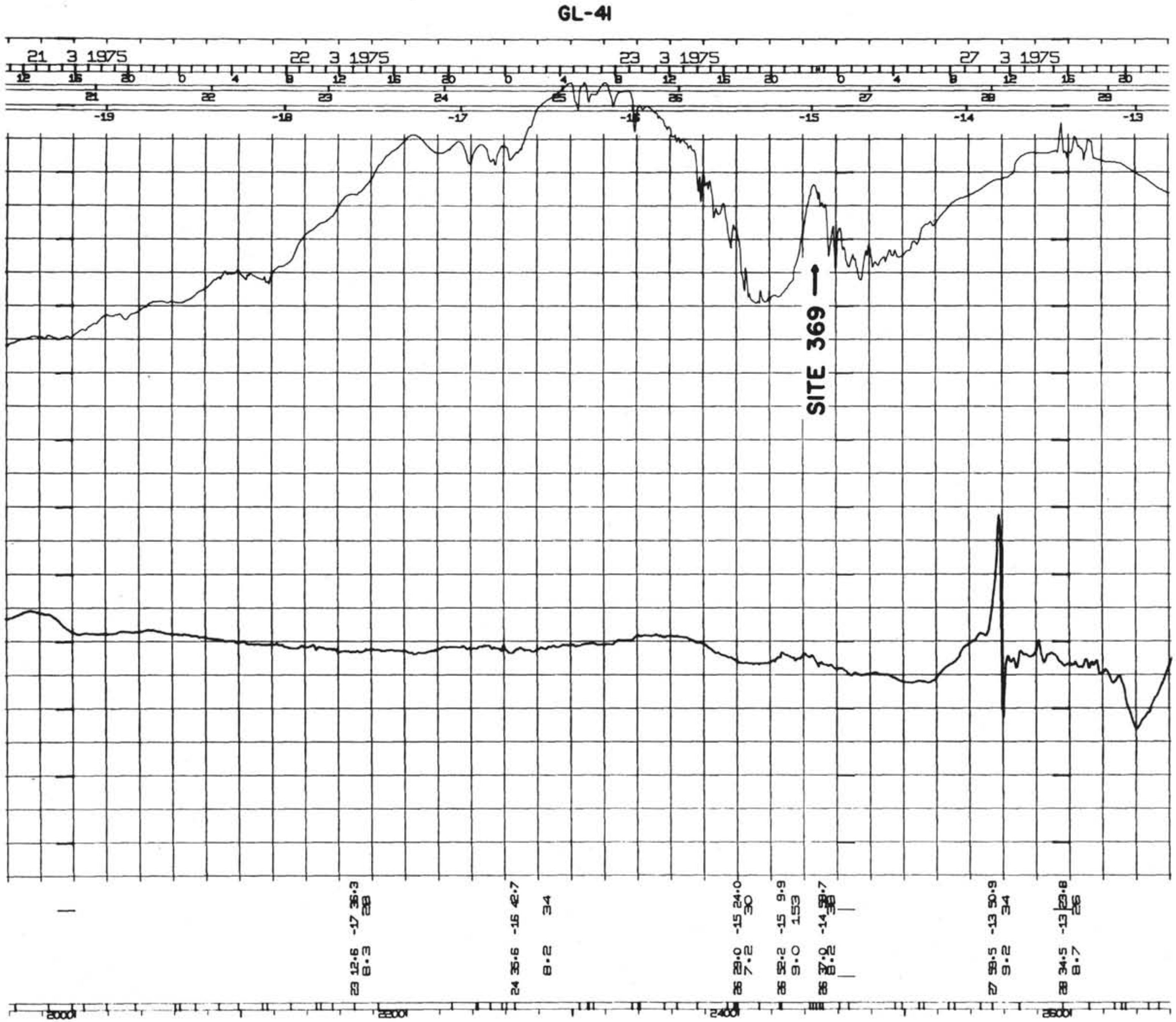

Figure 5. *Bathymetric and magnetic profiles along the track of Leg 41 of* Glomar Challenger. *Plots and scales explained in text.*

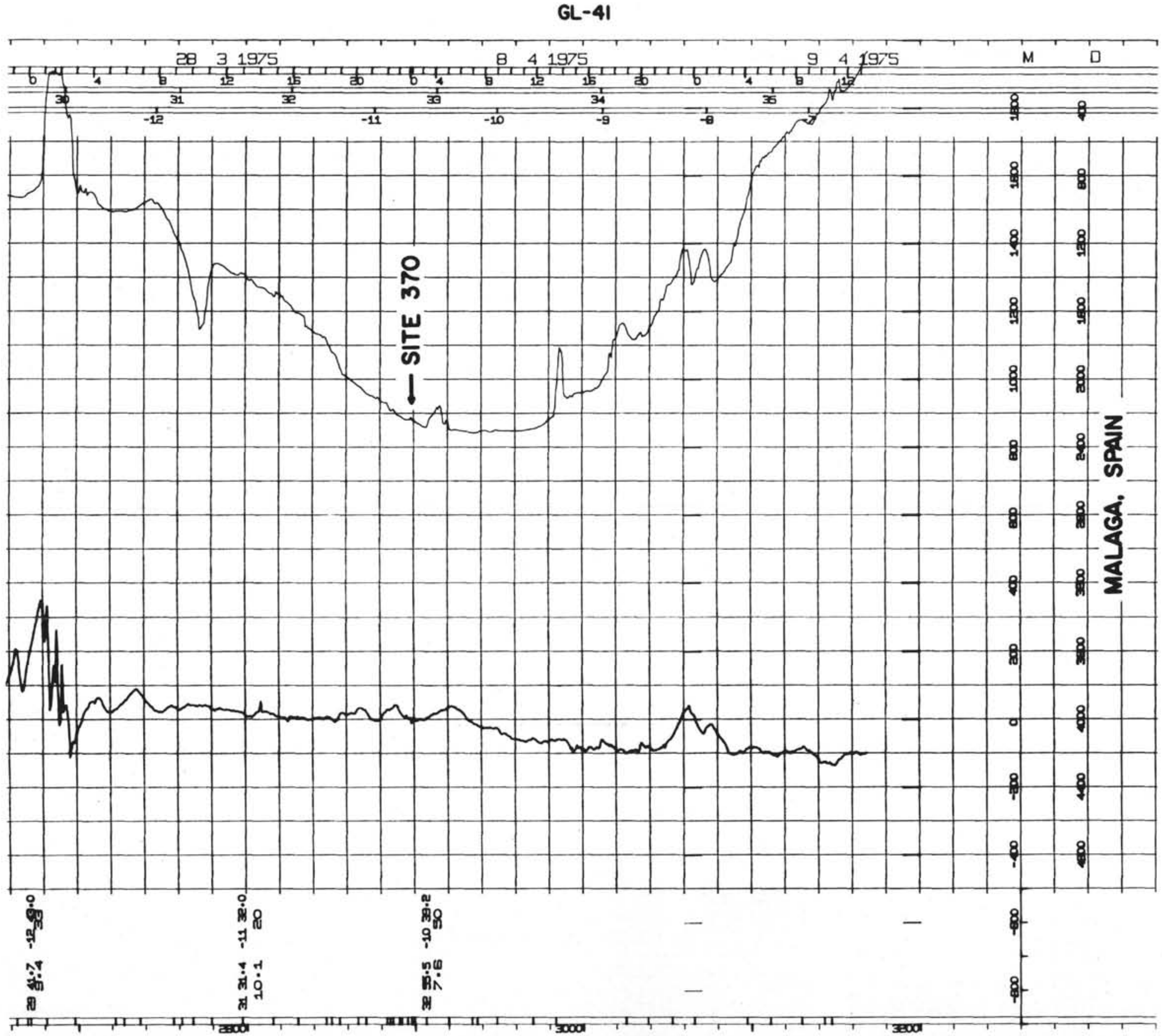

Figure 6. *Bathymetric and magnetic profiles along the track of Leg 41 of* Glomar Challenger. *Plots and scales explained in text.*

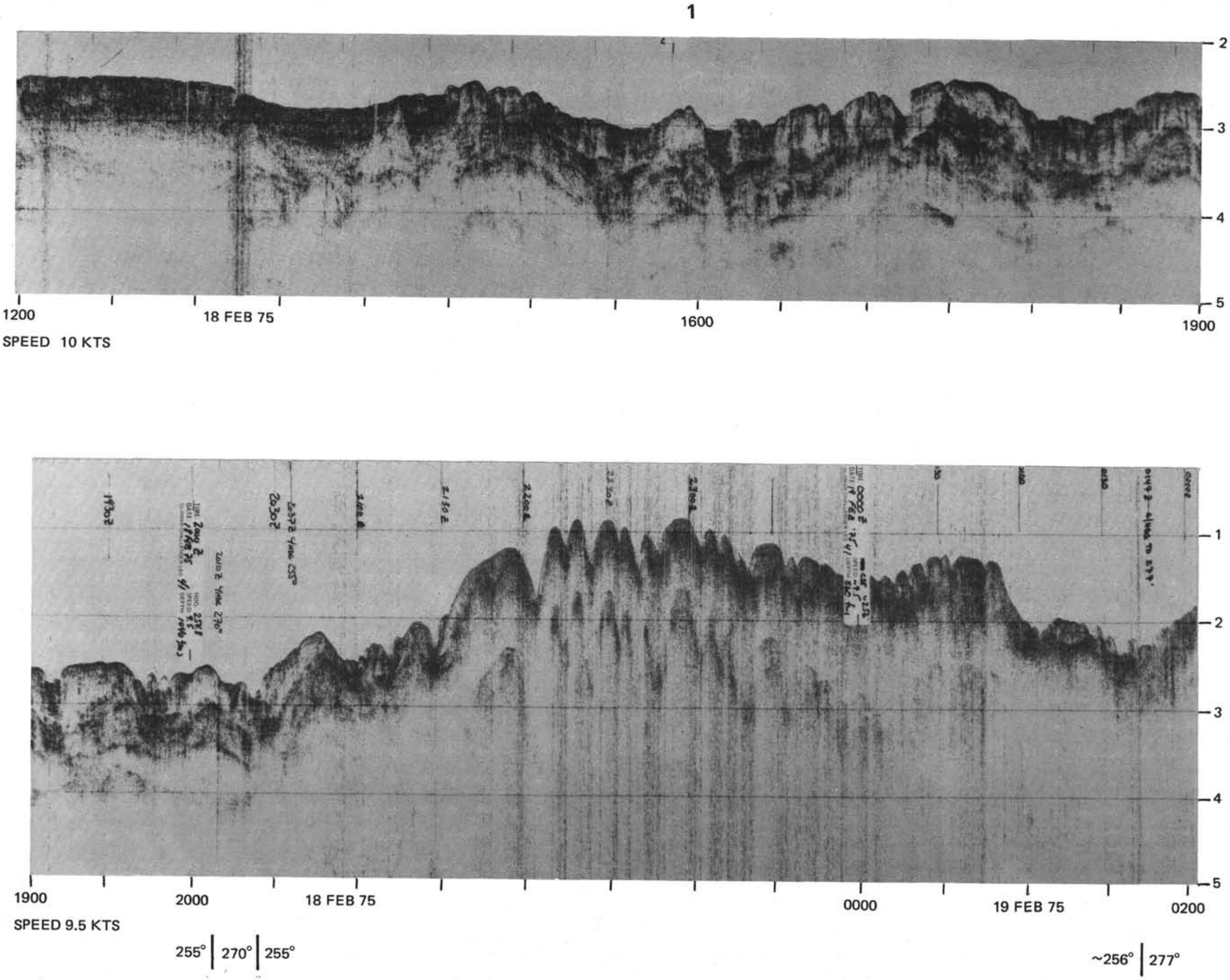

Figure 7. *Seismic profiles along the track of* Glomar Challenger.

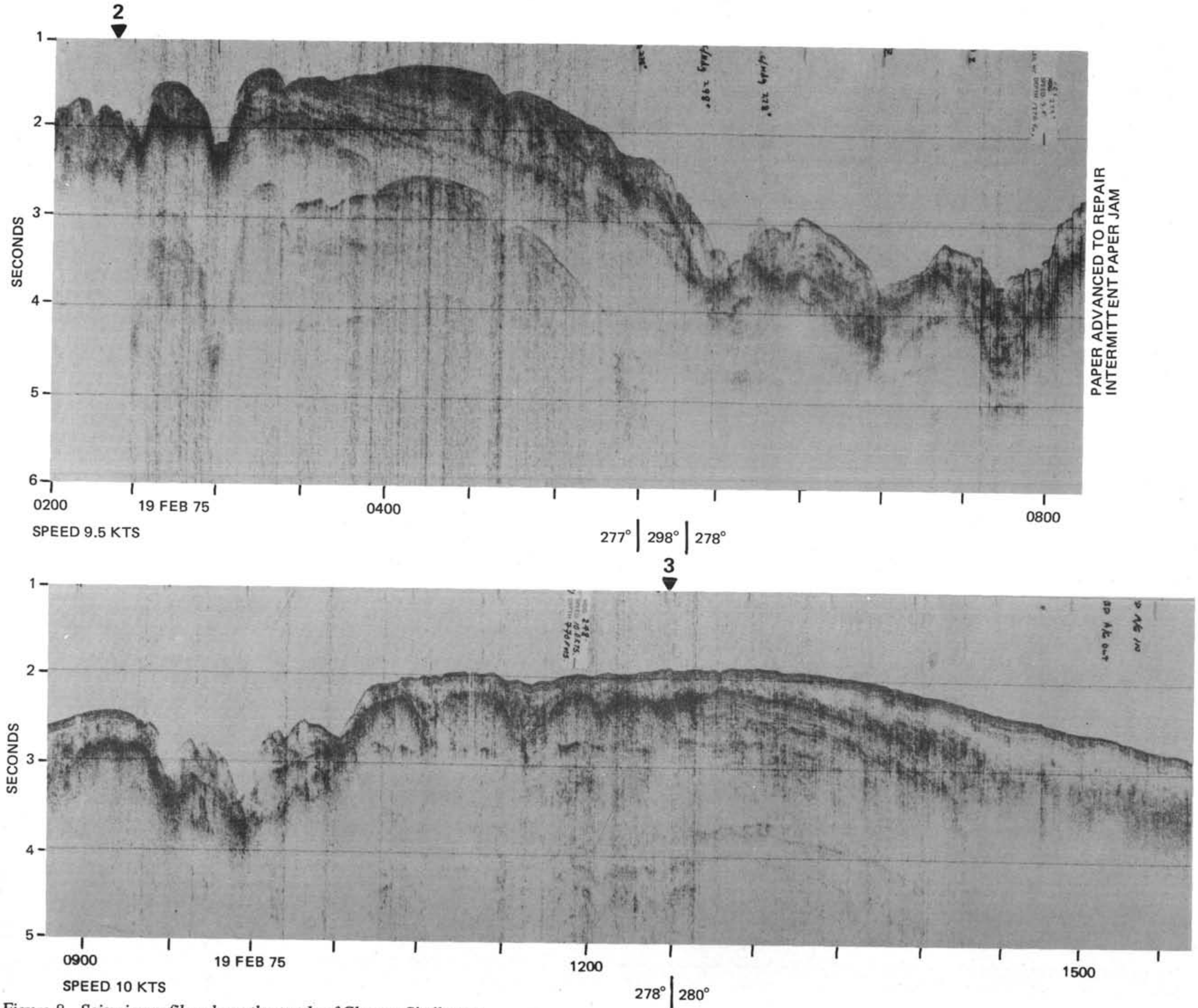

Figure 8. *Seismic profiles along the track of* Glomar Challenger.

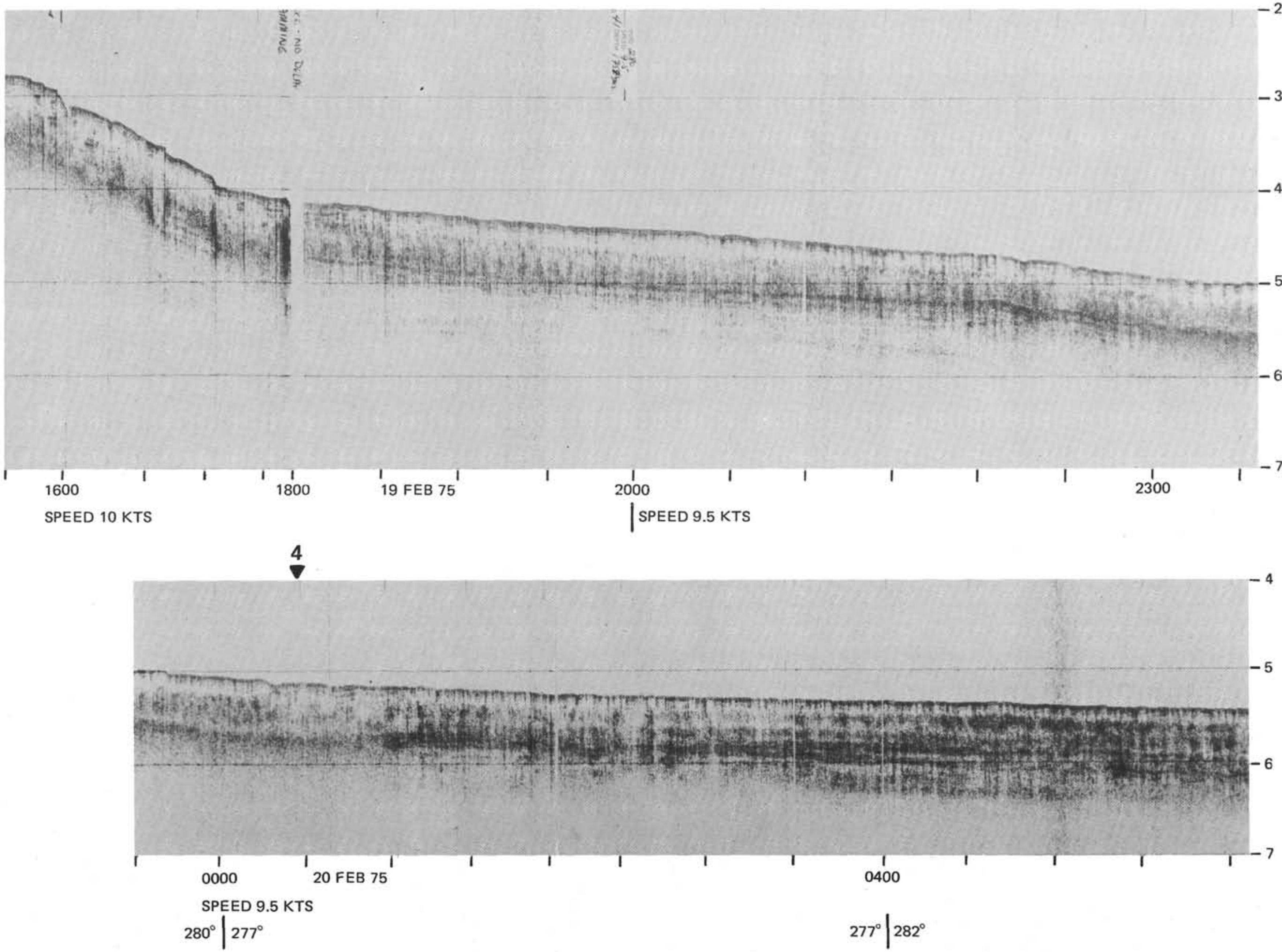

Figure 9. *Seismic profiles along the track of* Glomar Challenger.

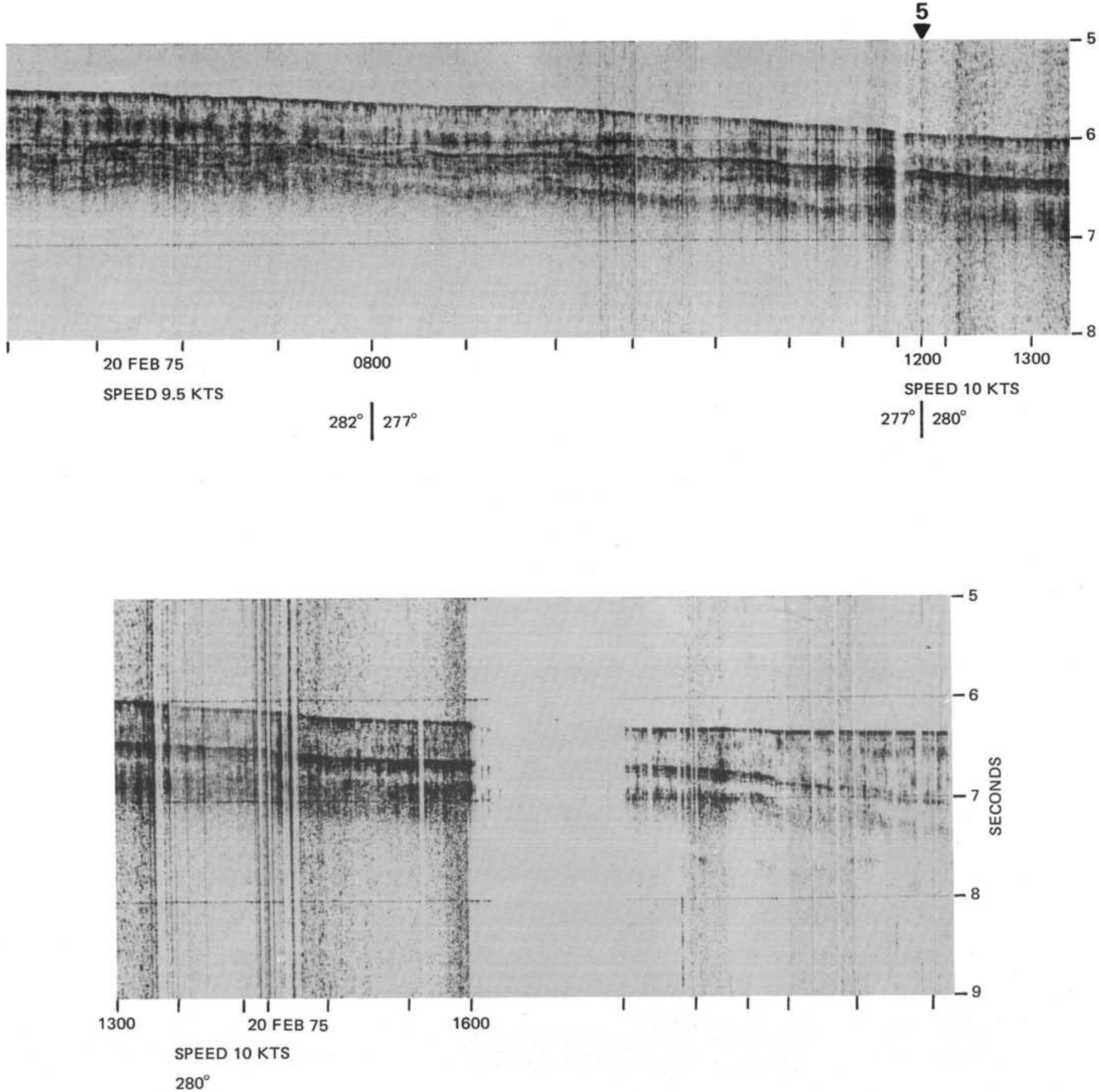

Figure 10. *Seismic profiles along the track of* Glomar Challenger.

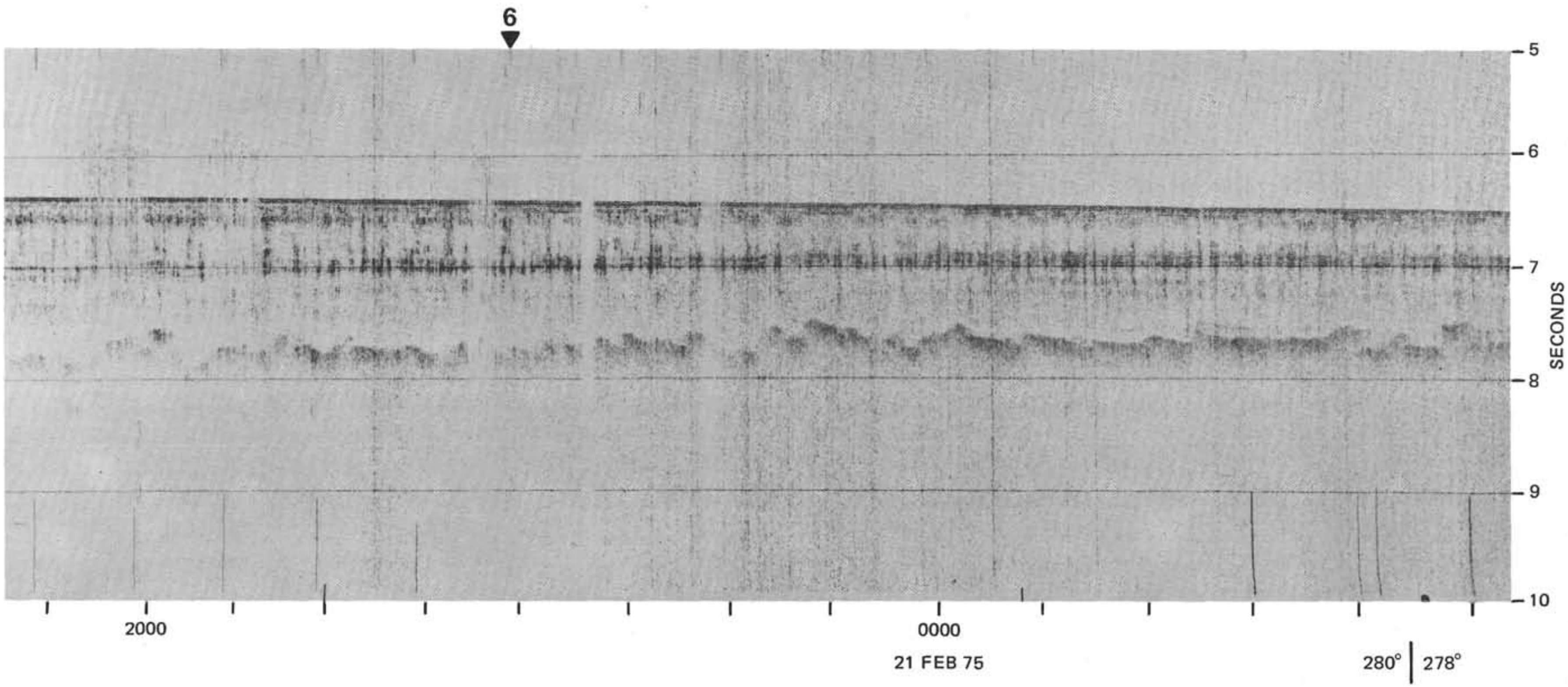

Figure 11. *Seismic profiles along the track of* Glomar Challenger.

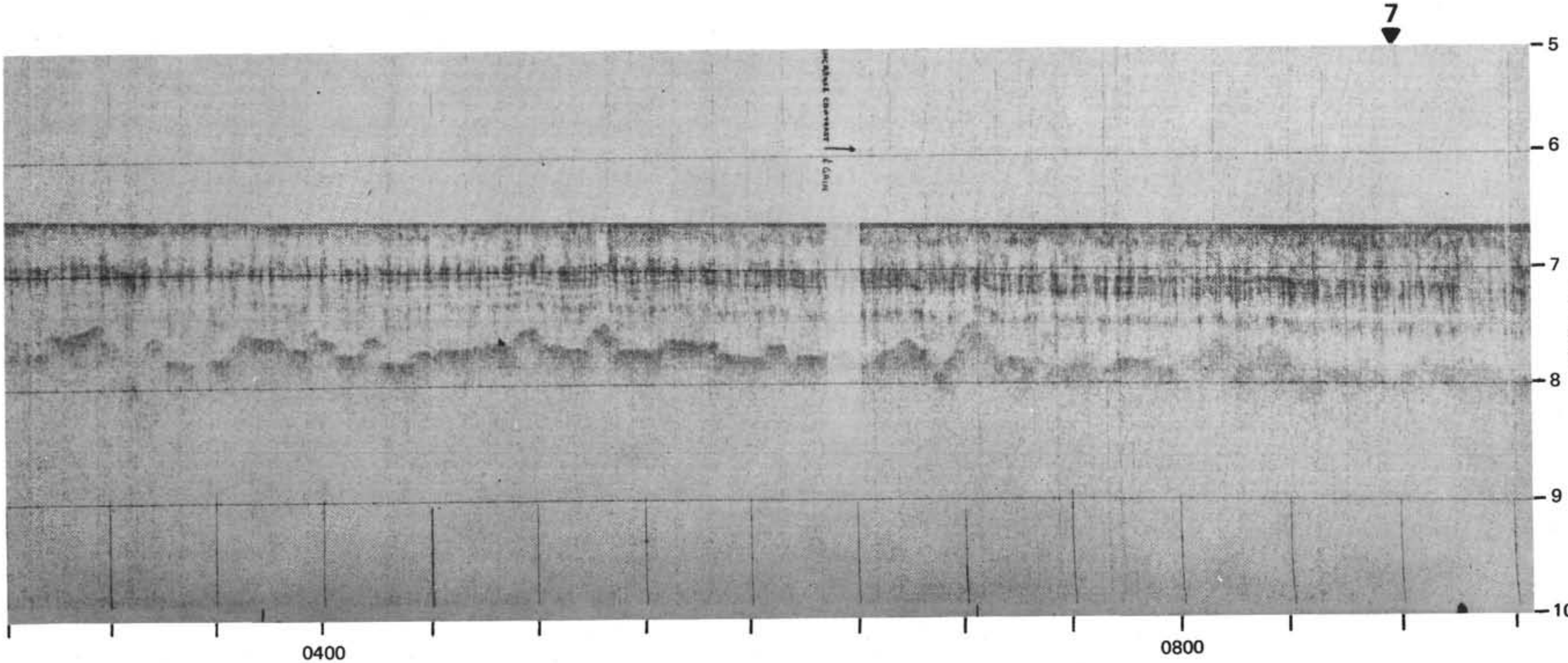

Figure 12. *Seismic profiles along the track of* Glomar Challenger.

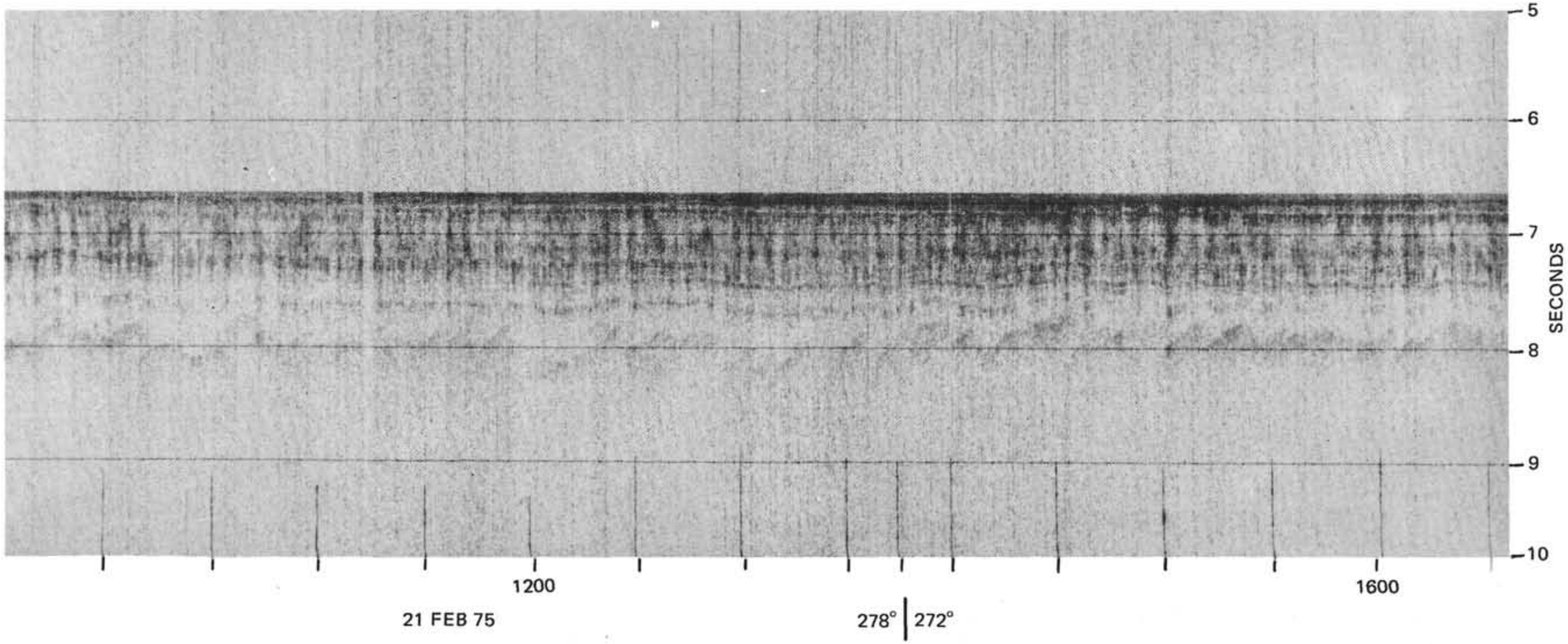

Figure 13. *Seismic profiles along the track of* Glomar Challenger.

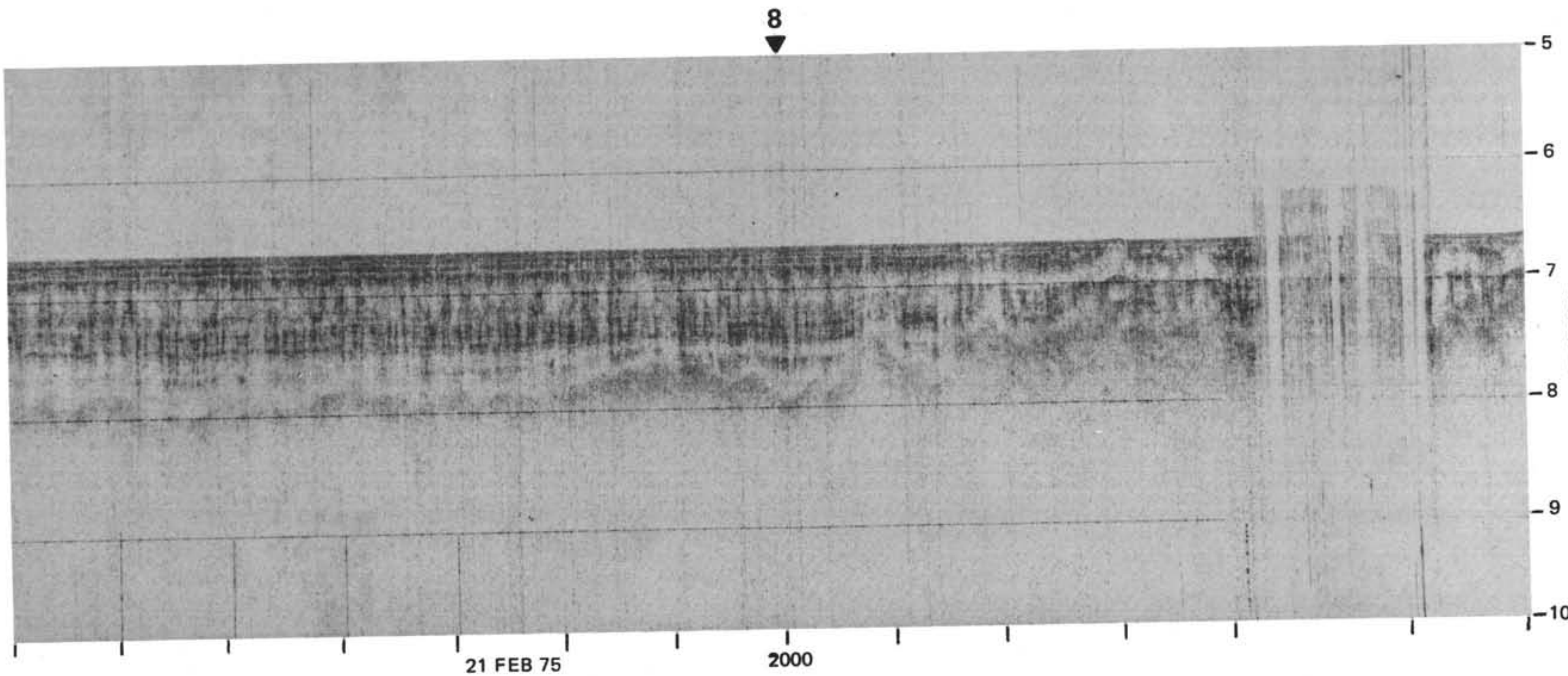

Figure 14. *Seismic profiles along the track of* Glomar Challenger.

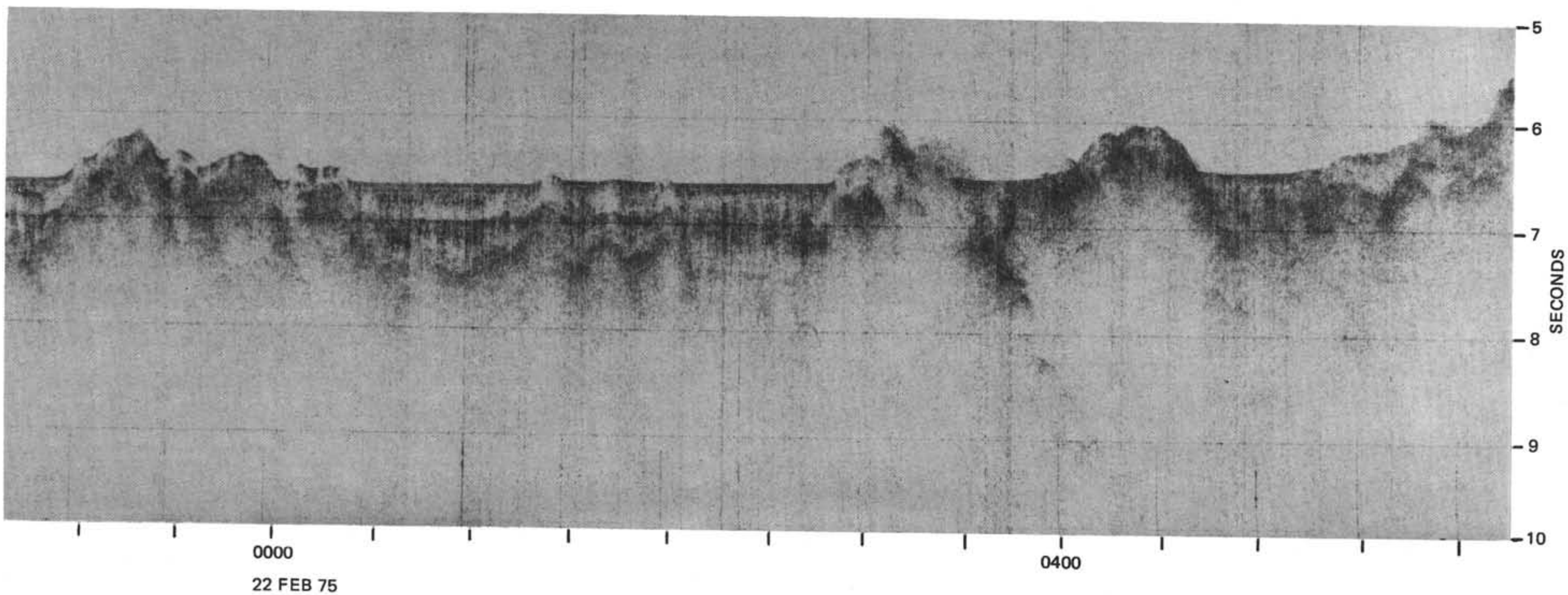

Figure 15. *Seismic profiles along the track of* Glomar Challenger.

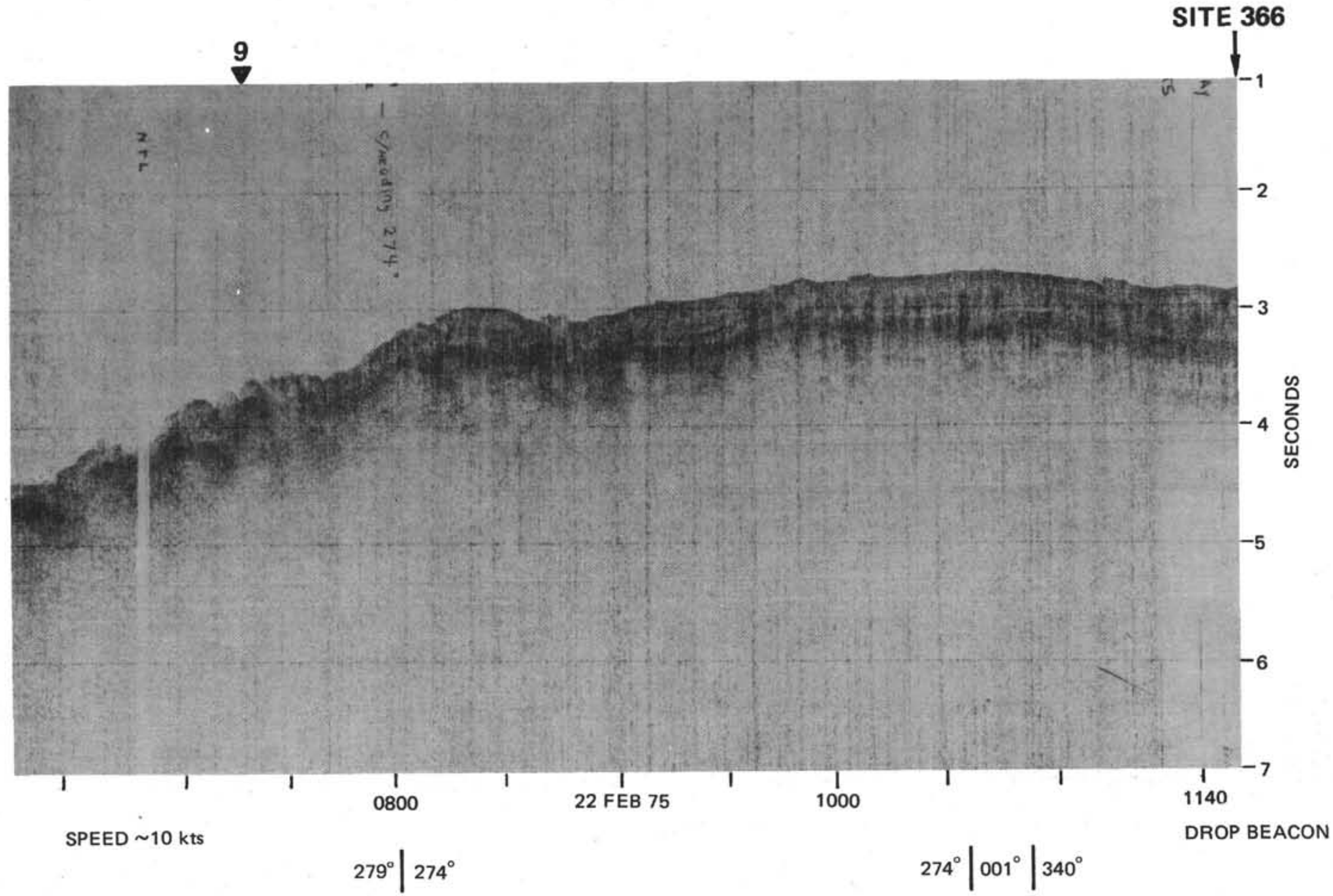

Figure 16. *Seismic profiles along the track of* Glomar Challenger.

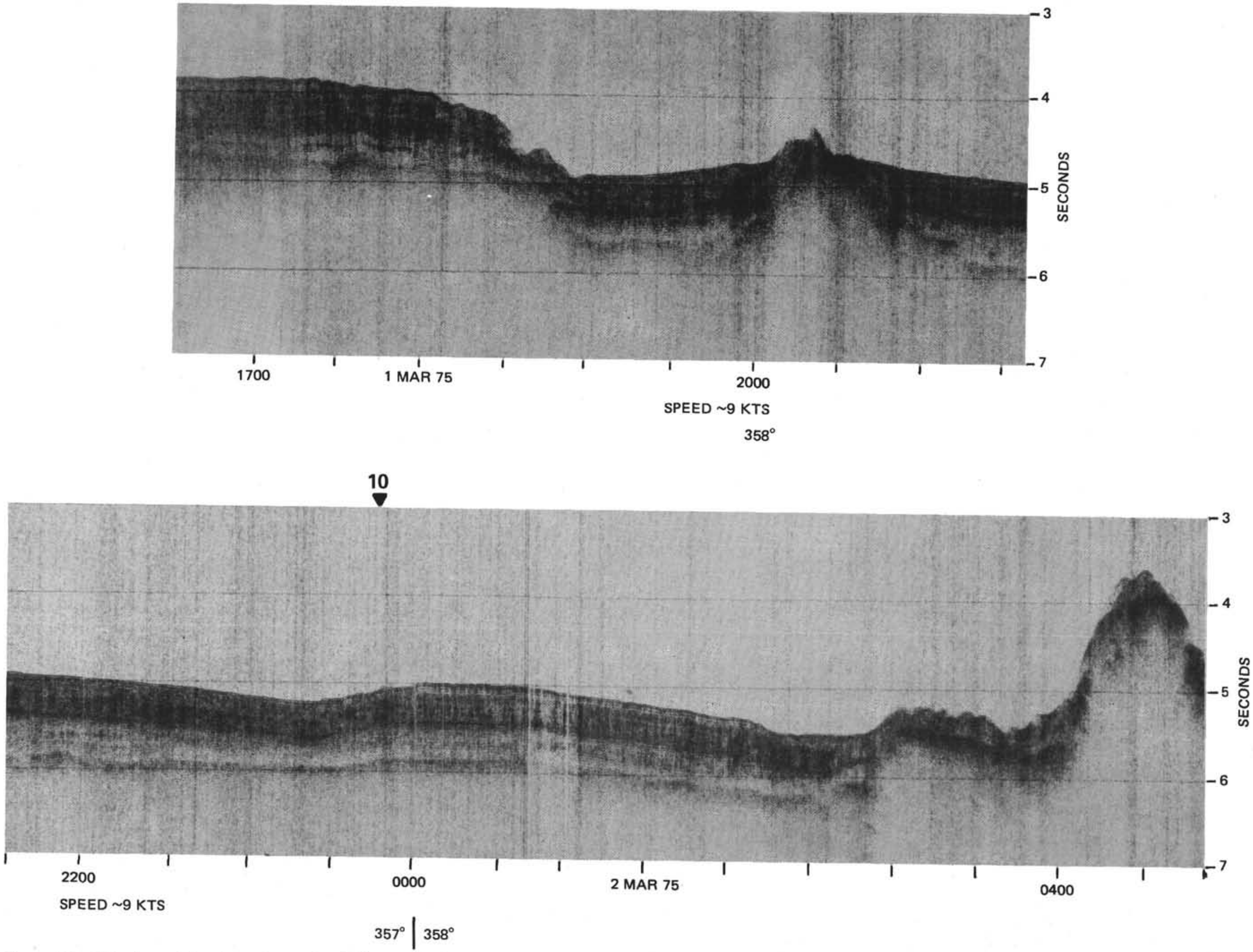

Figure 17. *Seismic profiles along the track of* Glomar Challenger.

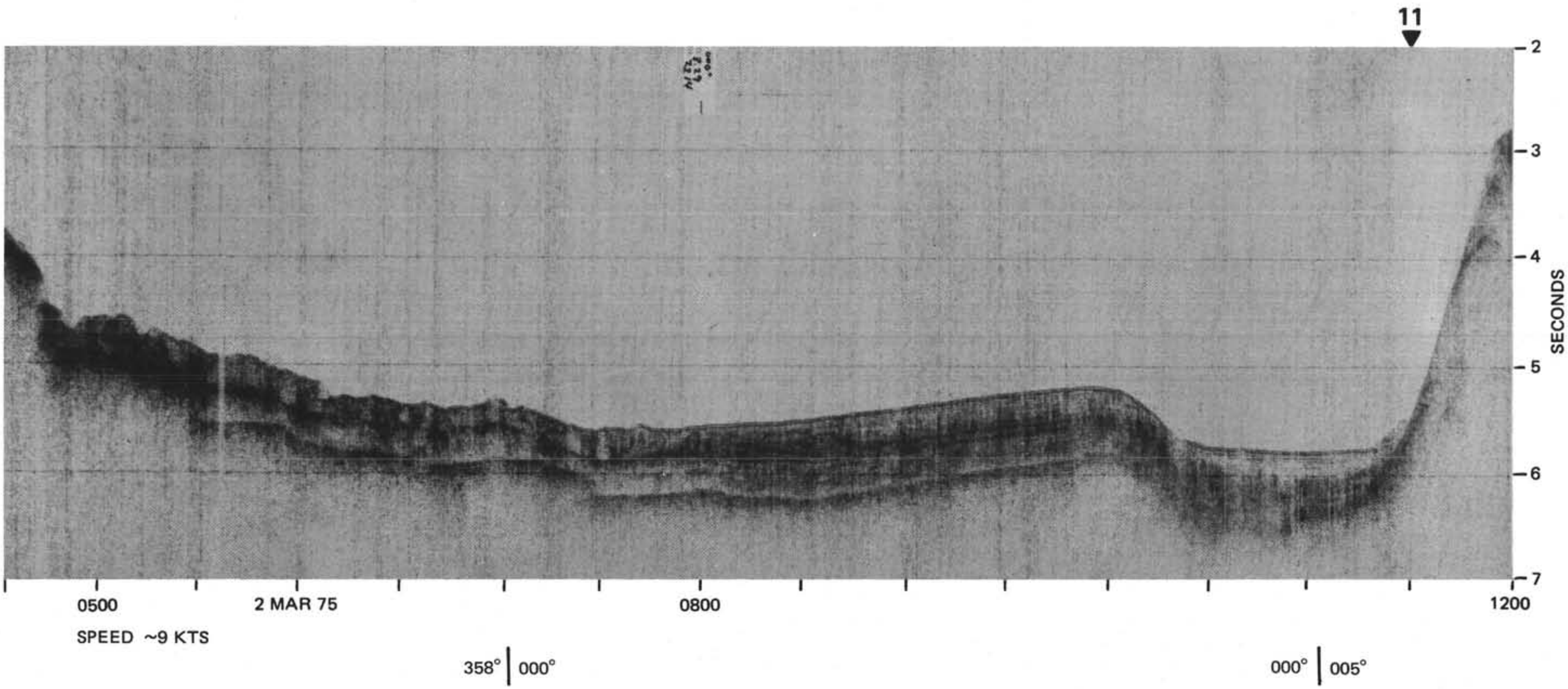

Figure 18. *Seismic profiles along the track of* Glomar Challenger.

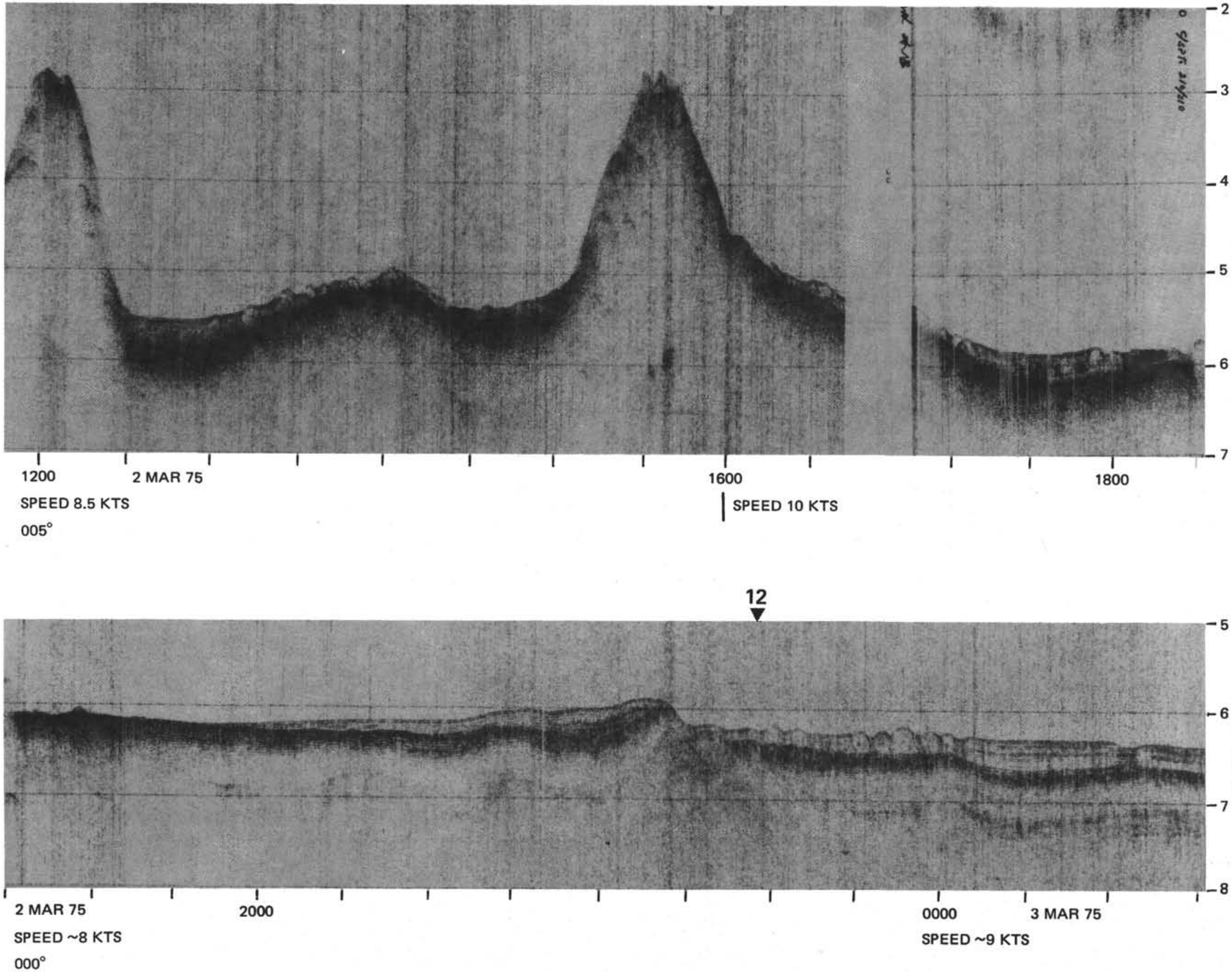

Figure 19. *Seismic profiles along the track of* Glomar Challenger.

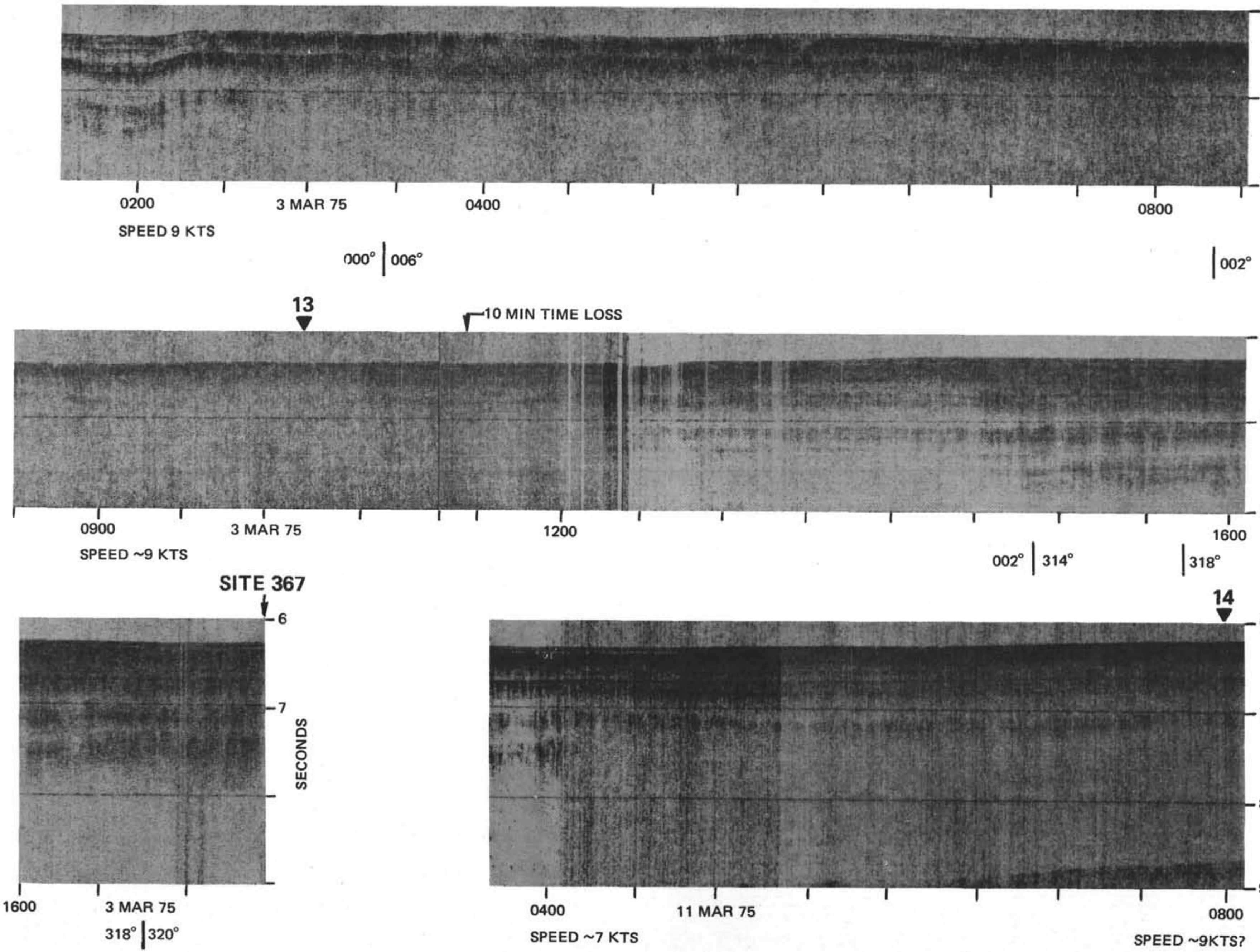

Figure 20. *Seismic profiles along the track of* Glomar Challenger.

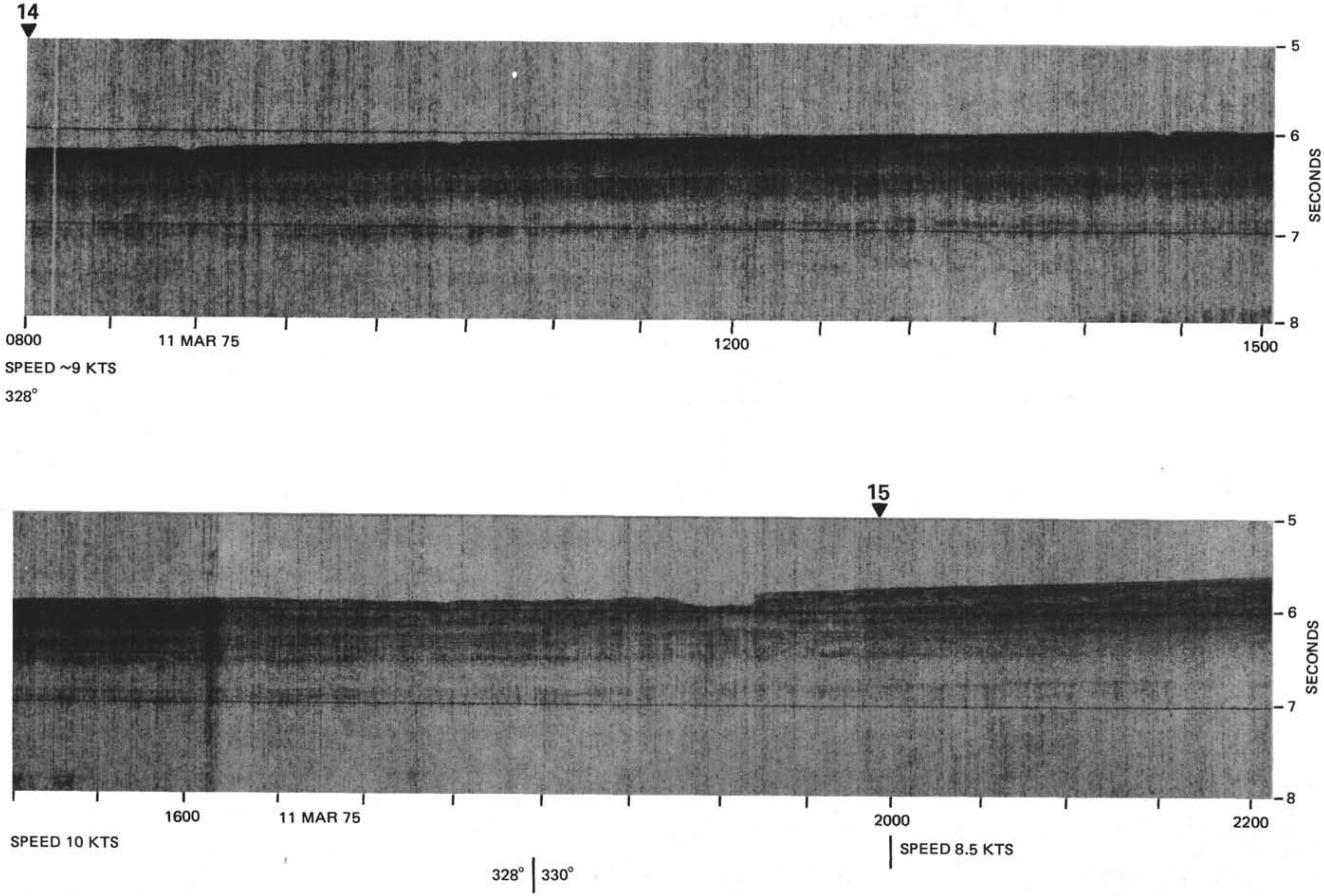

Figure 21. *Seismic profiles along the track of* Glomar Challenger.

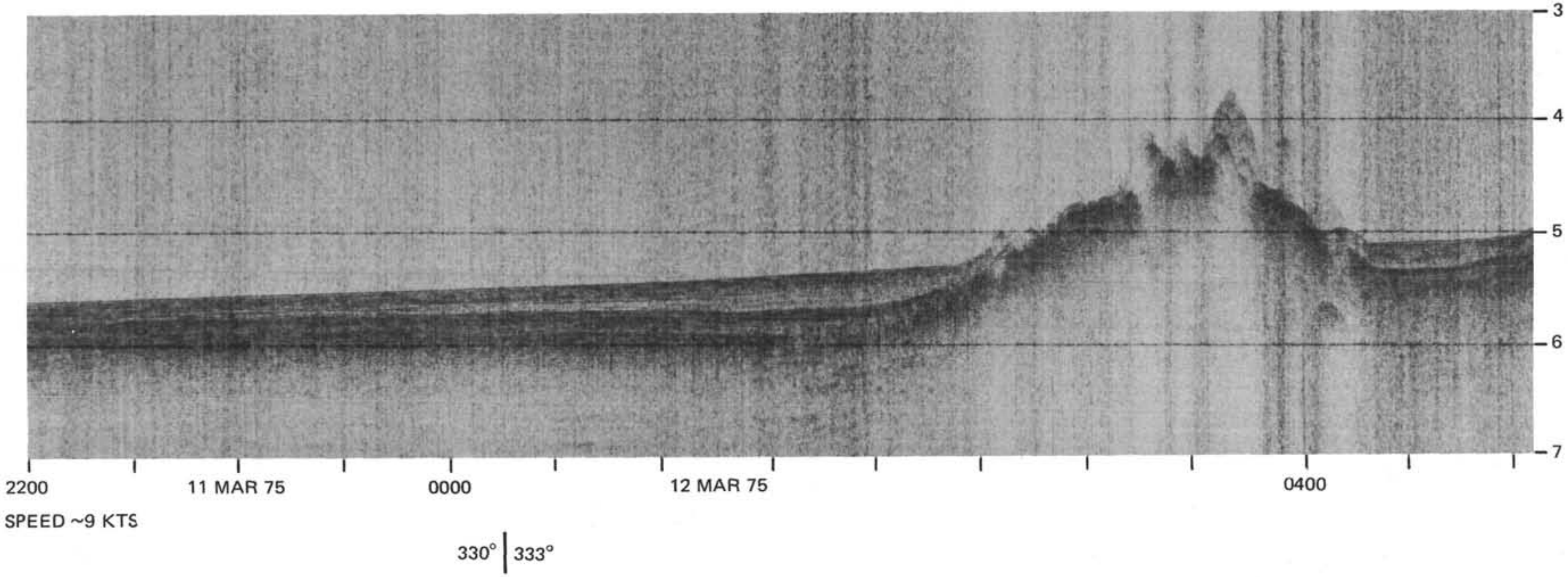

Figure 22. *Seismic profiles along the track of* Glomar Challenger.

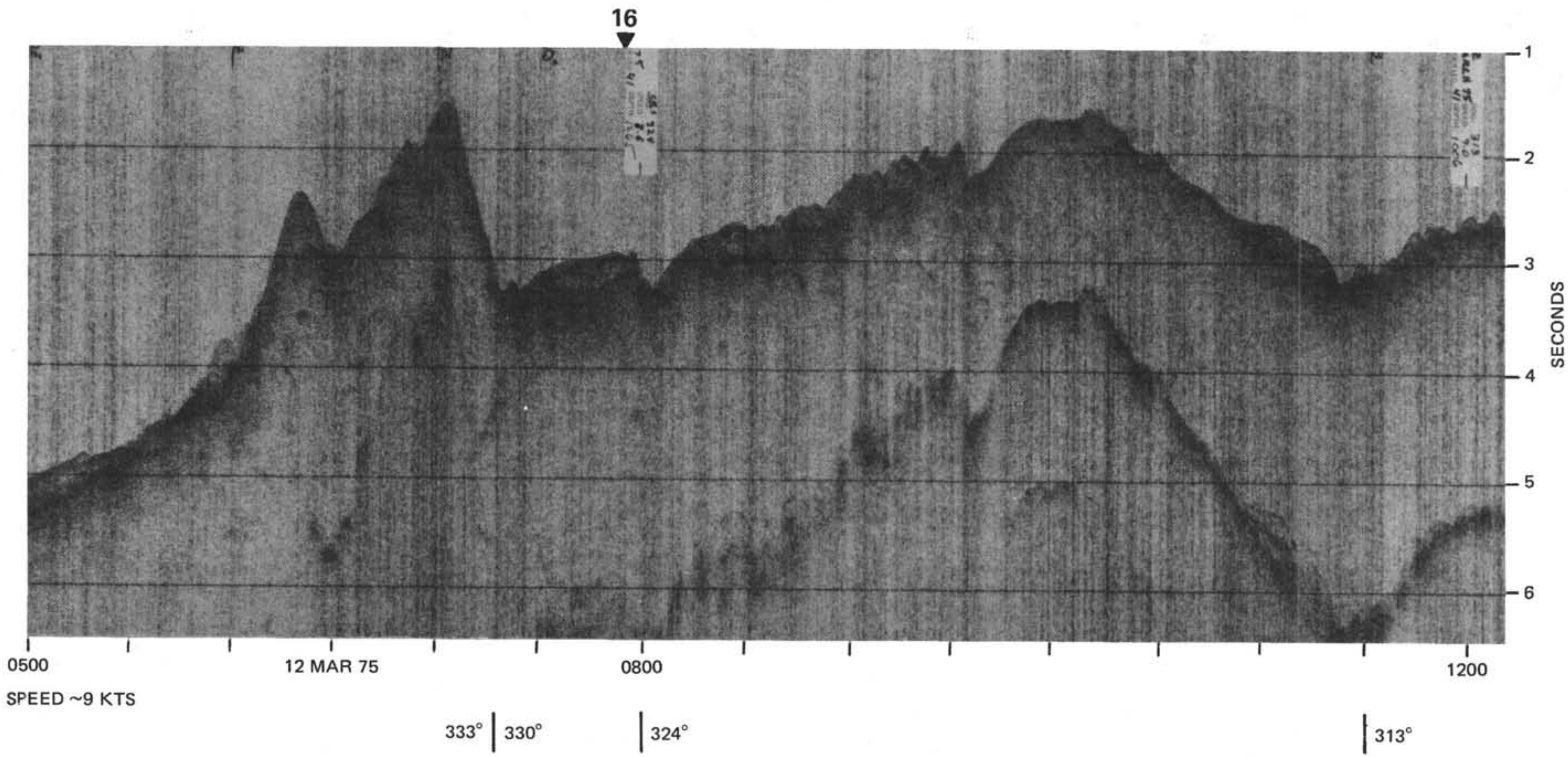

Figure 23. *Seismic profiles along the track of* Glomar Challenger.

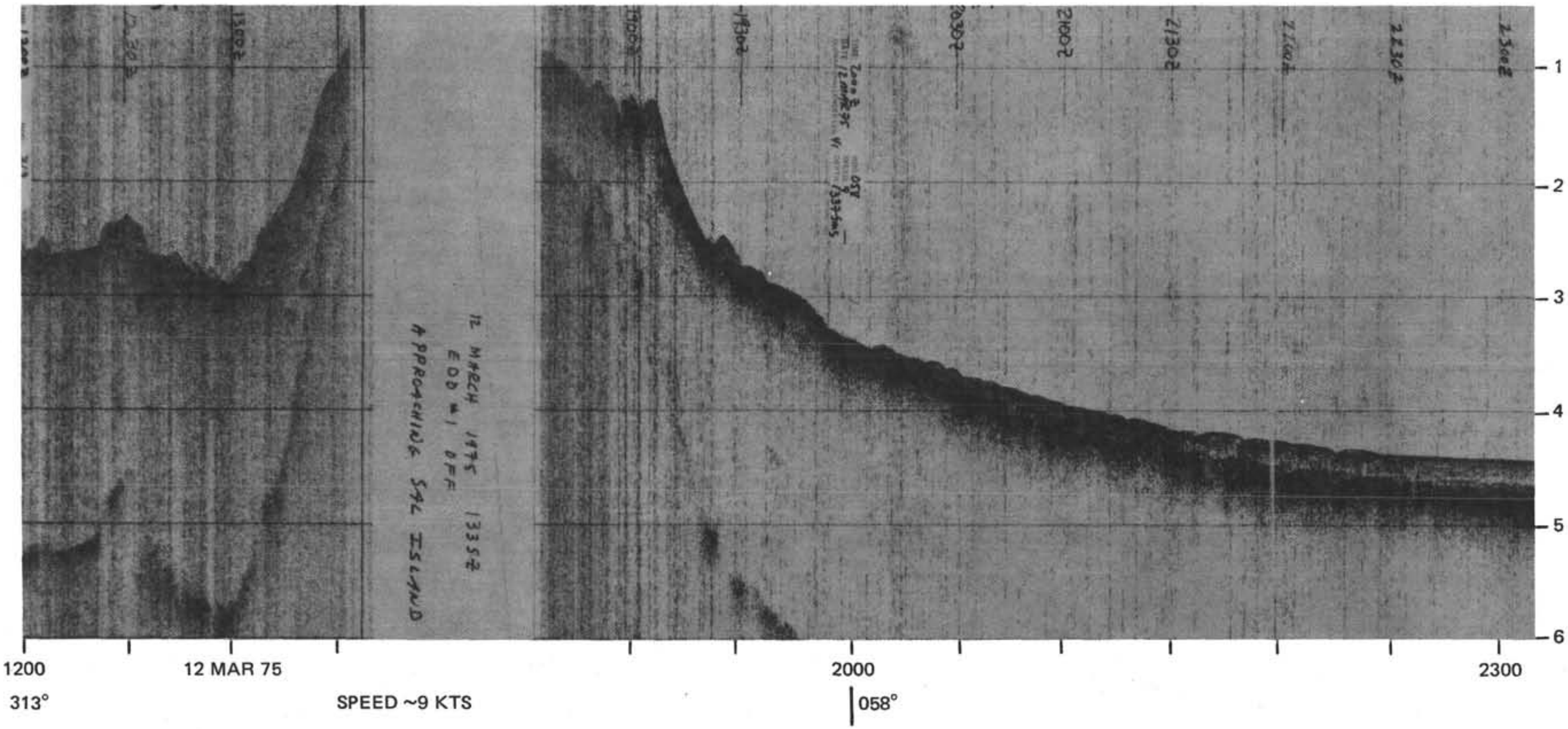

Figure 24. *Seismic profiles along the track of* Glomar Challenger.

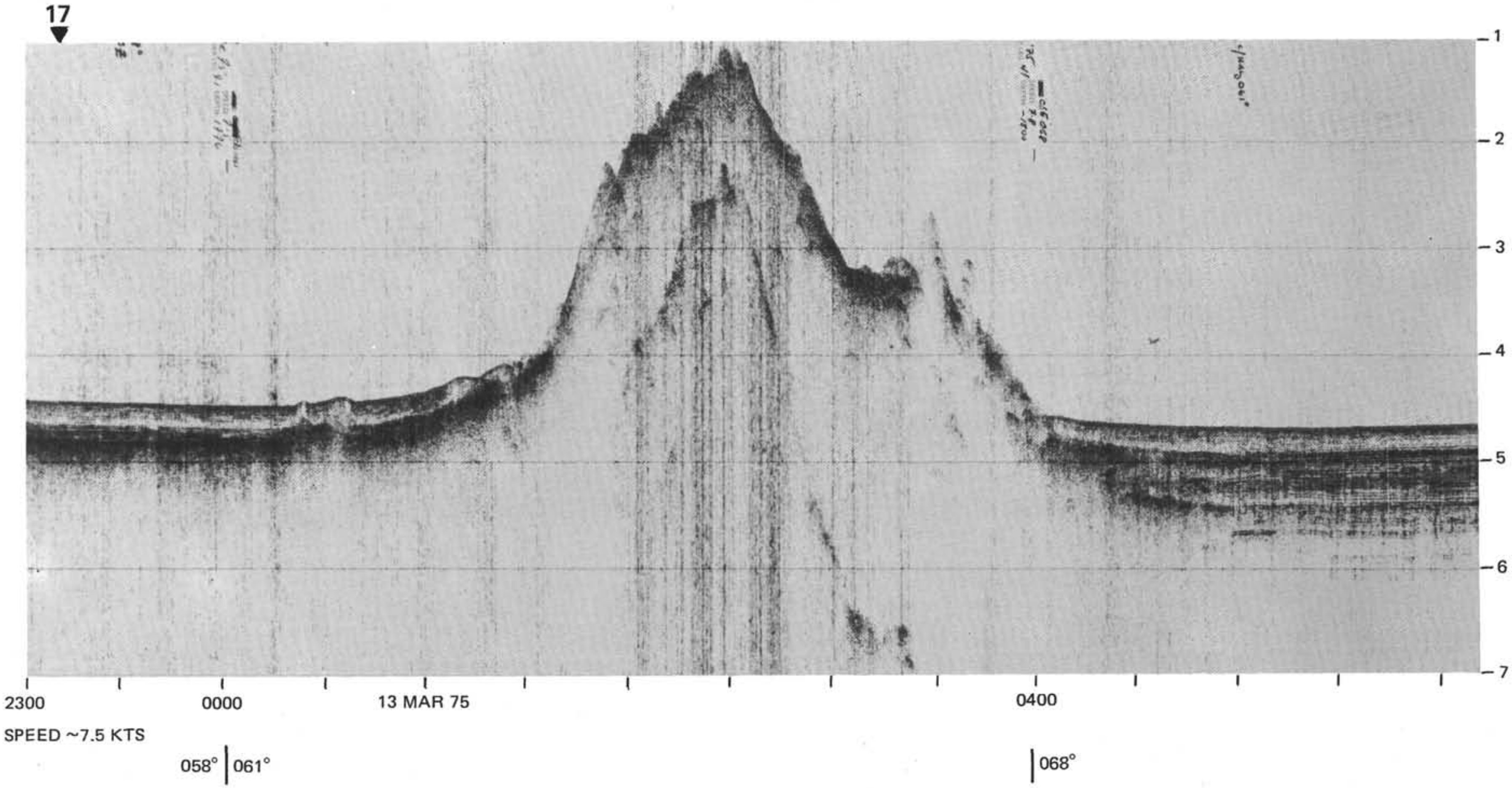

Figure 25. *Seismic profiles along the track of* Glomar Challenger.

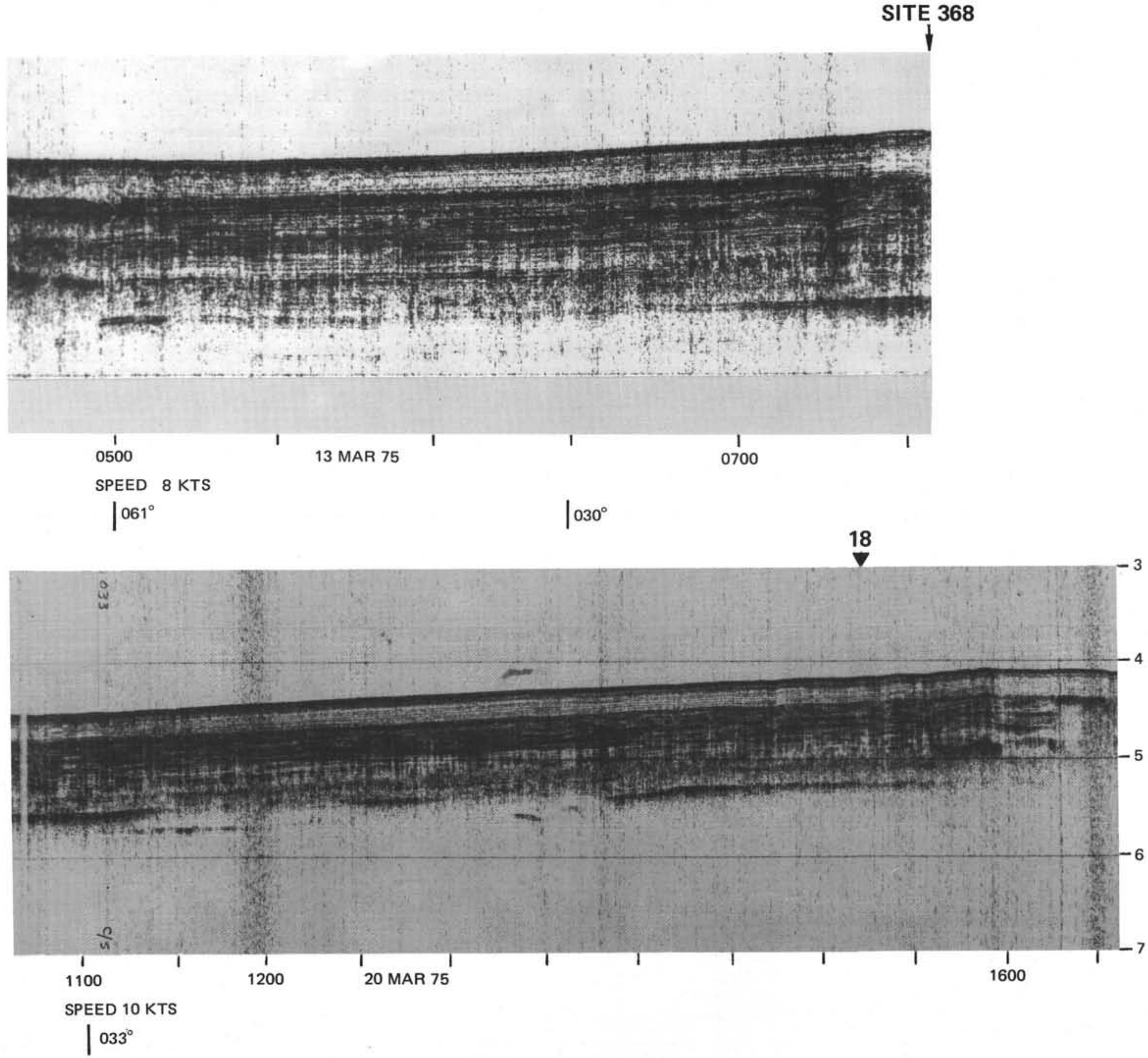

Figure 26. *Seismic profiles along the track of* Glomar Challenger.

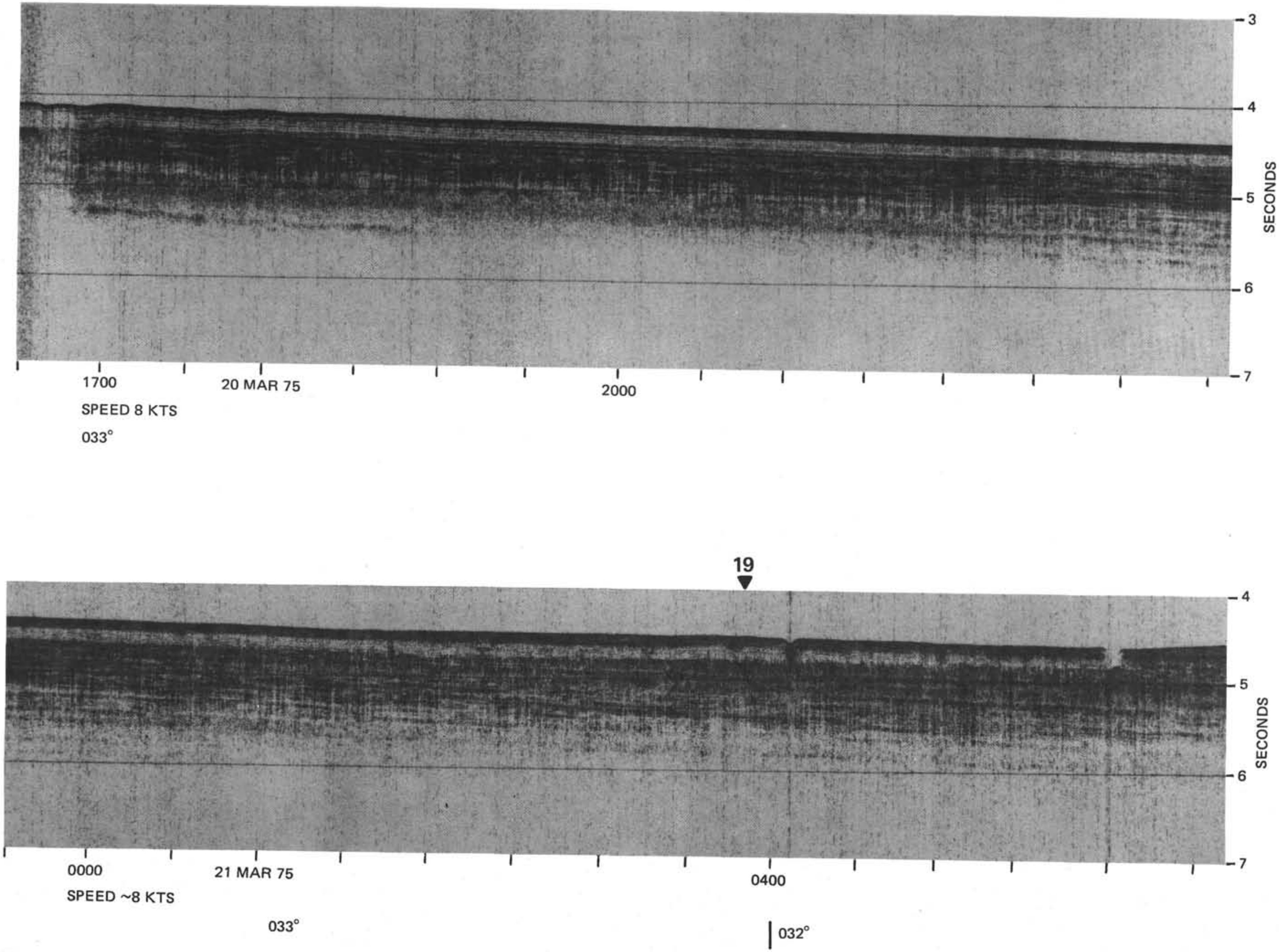

Figure 27. *Seismic profiles along the track of* Glomar Challenger.

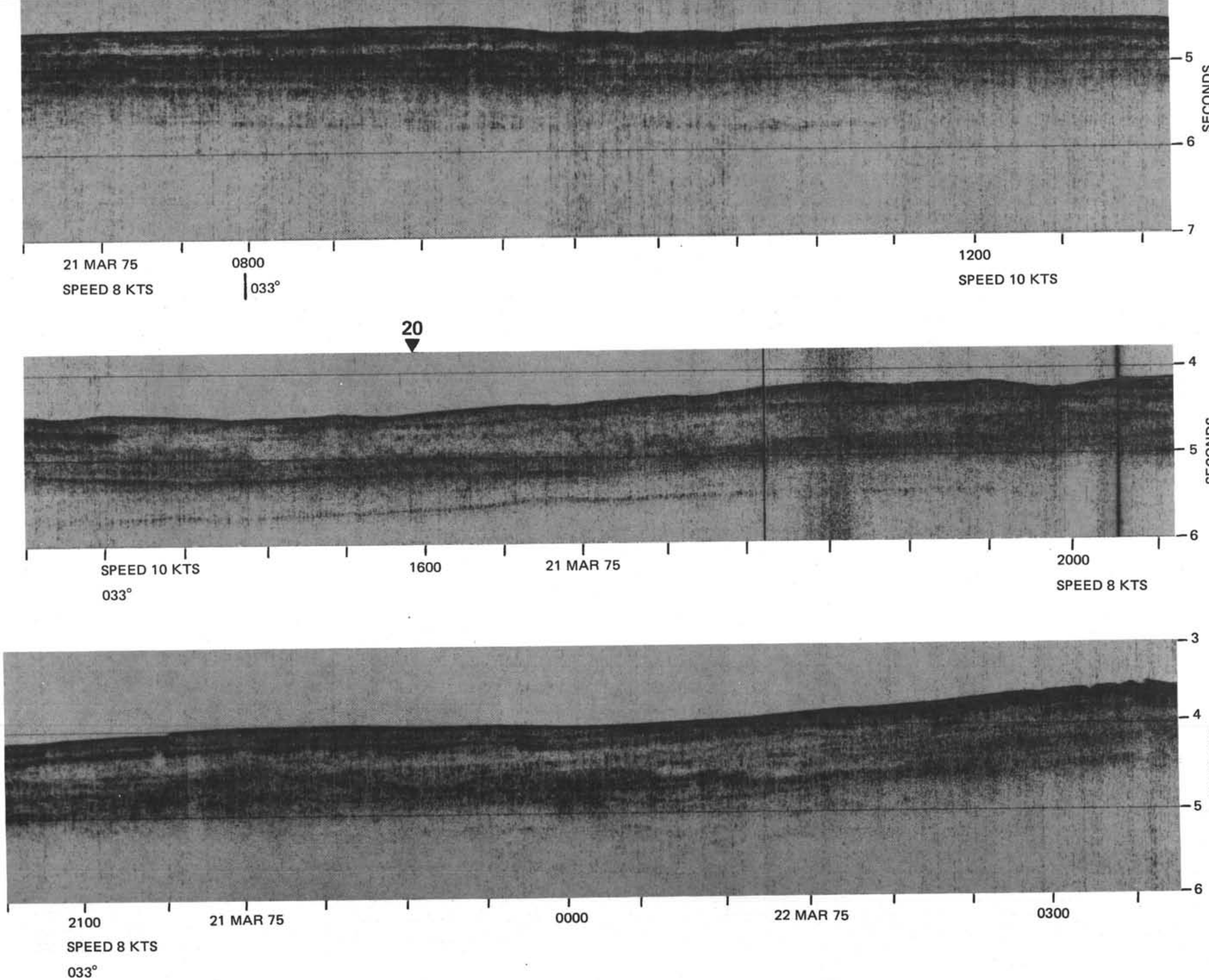

Figure 28. *Seismic profiles along the track of* Glomar Challenger.

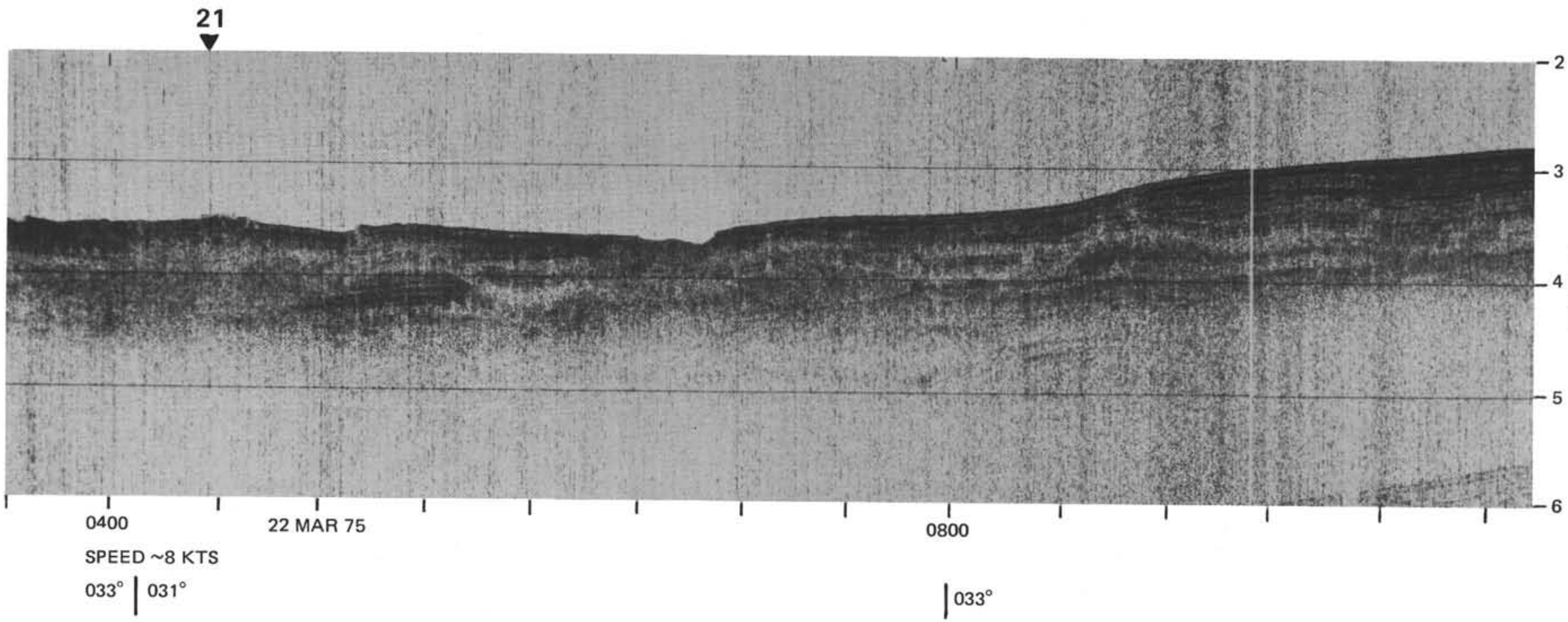

Figure 29. *Seismic profiles along the track of* Glomar Challenger.

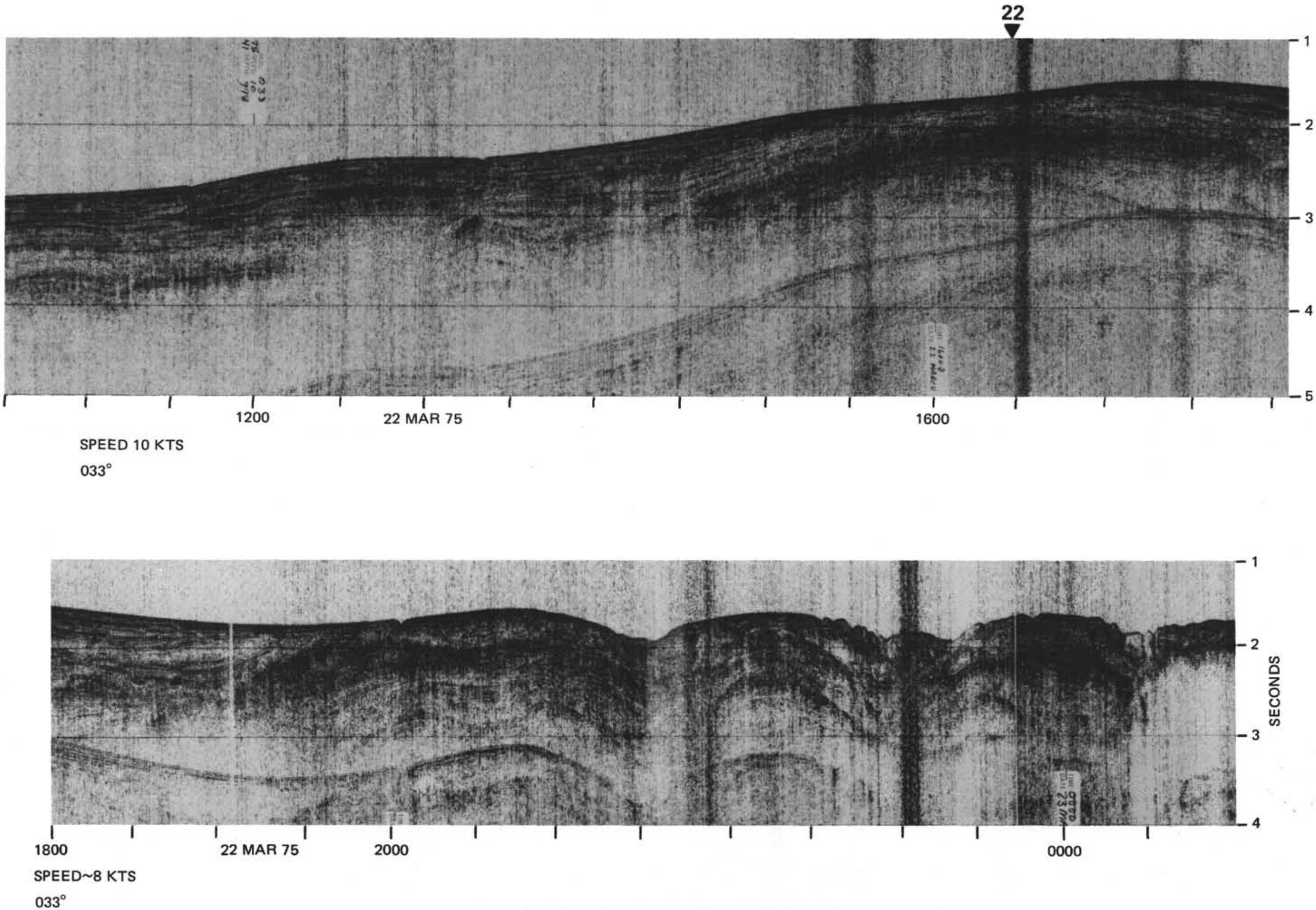

Figure 30. *Seismic profiles along the track of* Glomar Challenger.

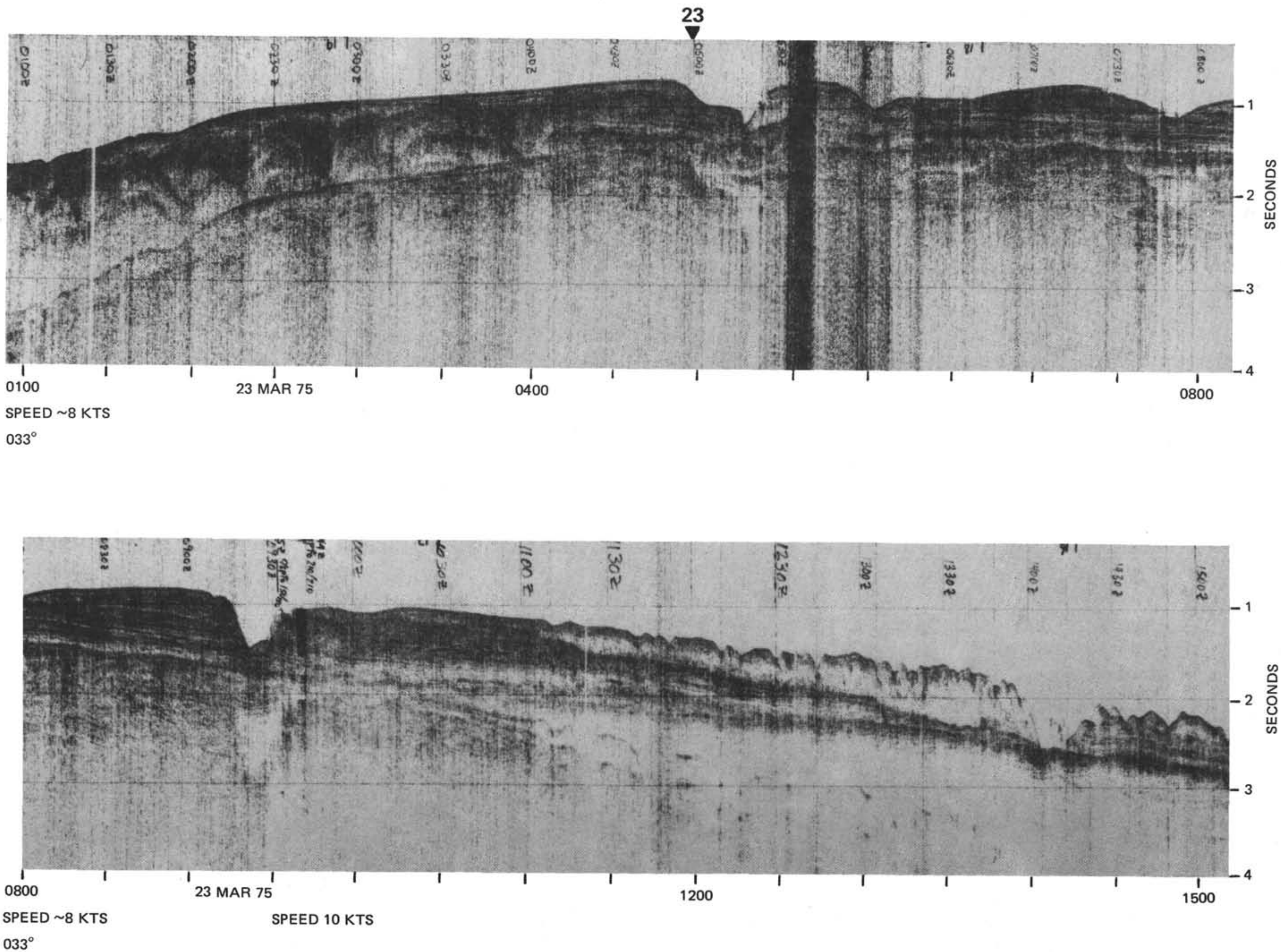

Figure 31. *Seismic profiles along the track of* Glomar Challenger.

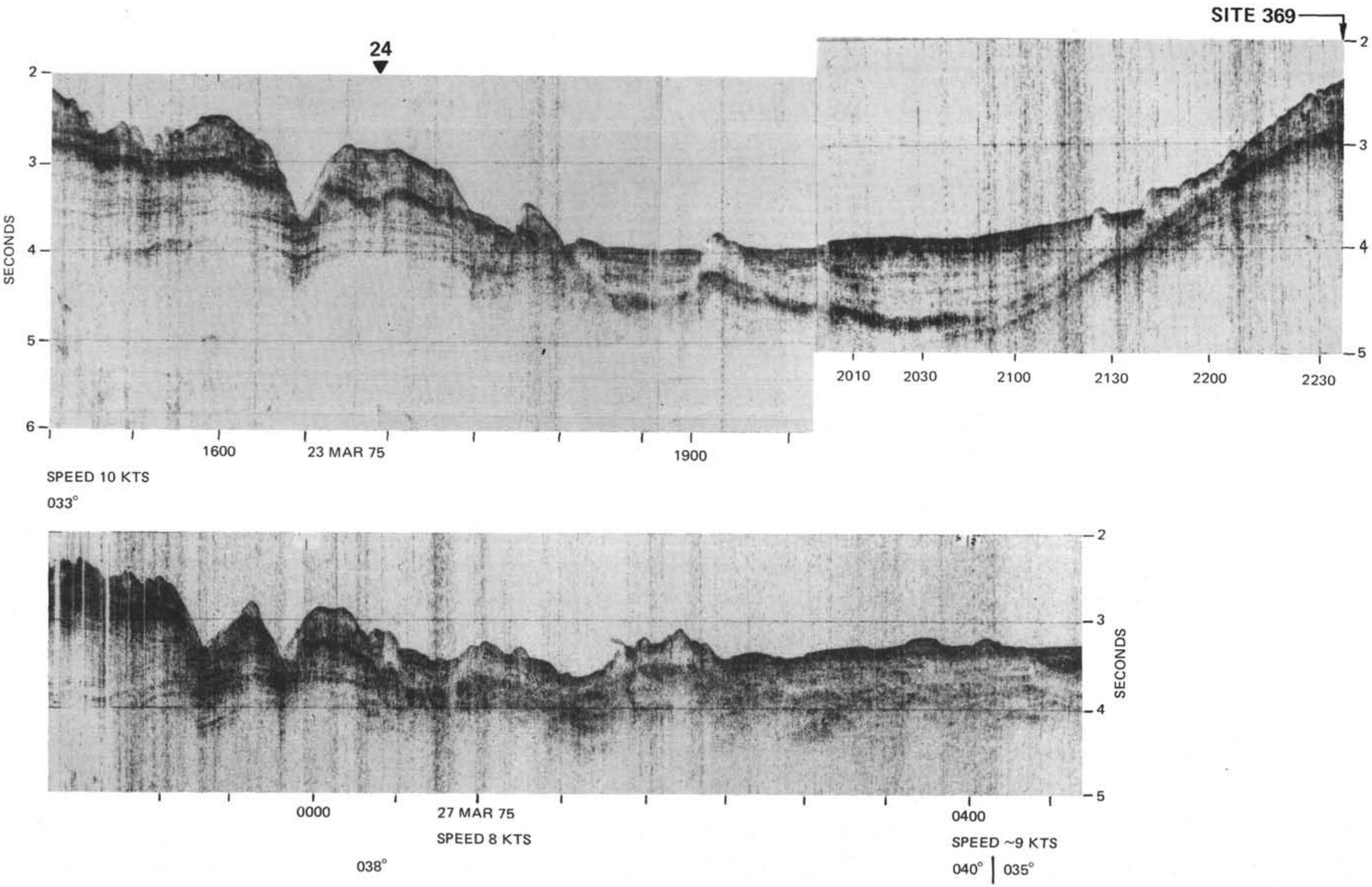

Figure 32. *Seismic profiles along the track of* Glomar Challenger.

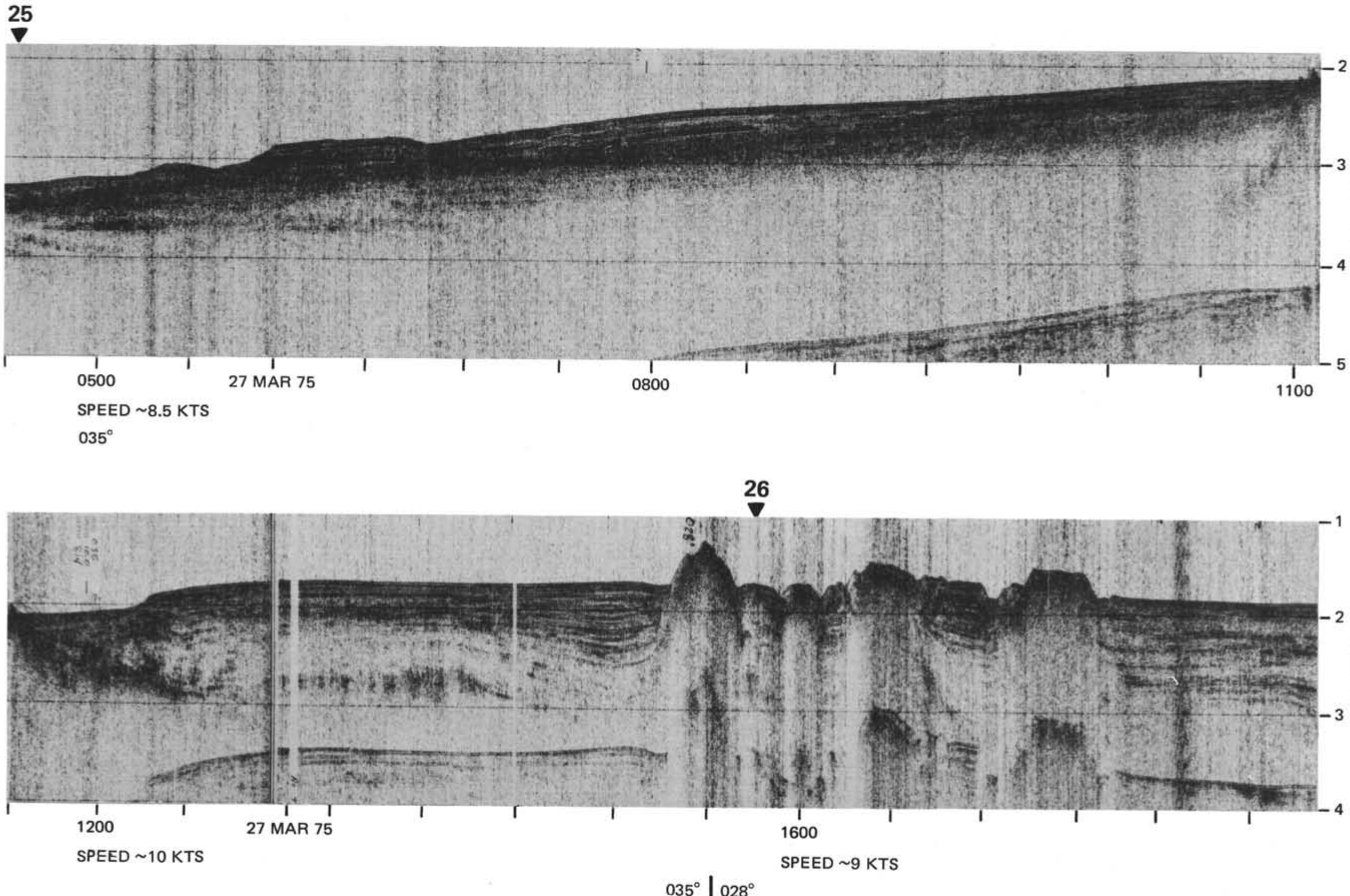

Figure 33. *Seismic profiles along the track of* Glomar Challenger.

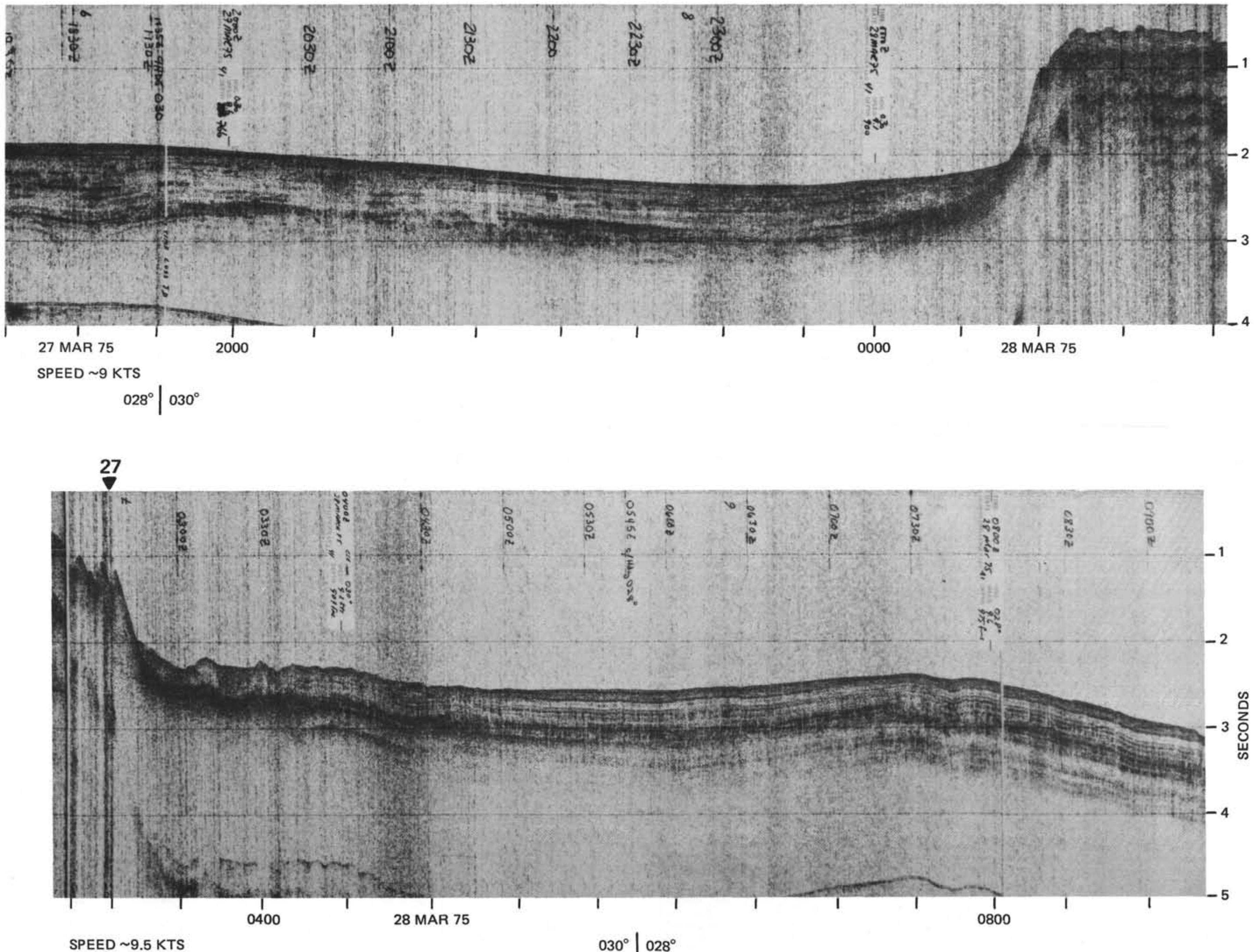

Figure 34. *Seismic profiles along the track of* Glomar Challenger.

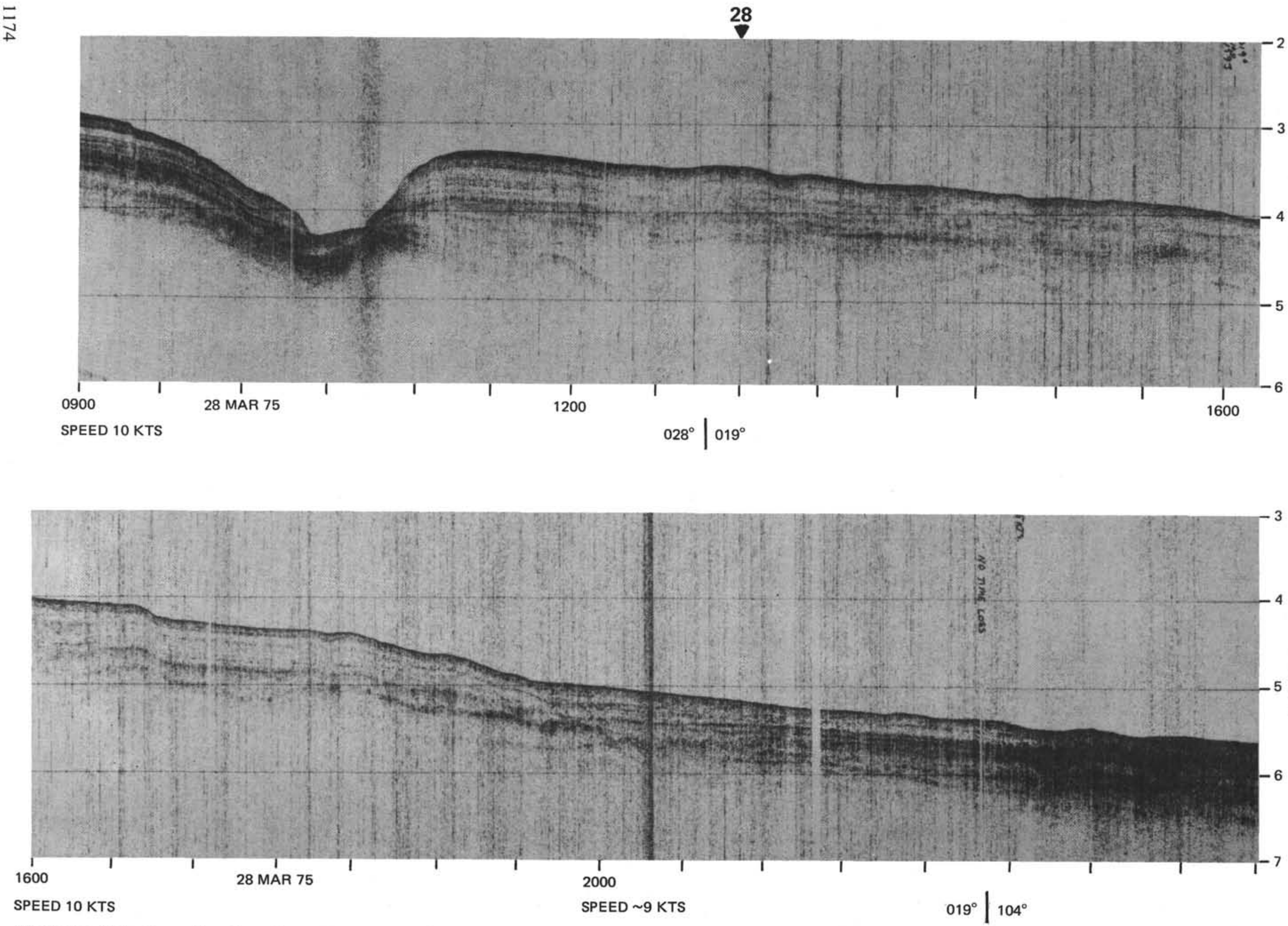

Figure 35. *Seismic profiles along the track of* Glomar Challenger.

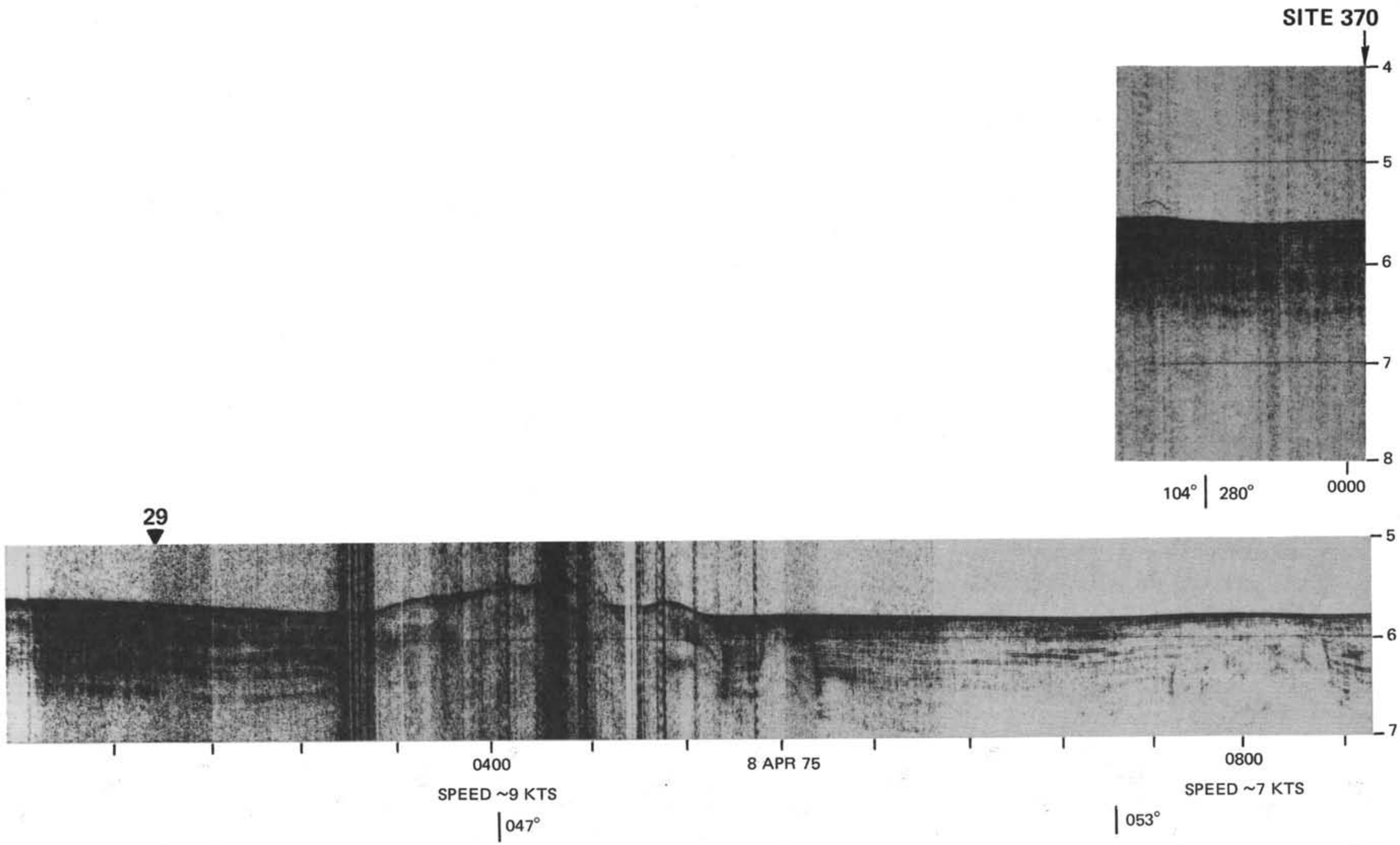

Figure 36. *Seismic profiles along the track of* Glomar Challenger.

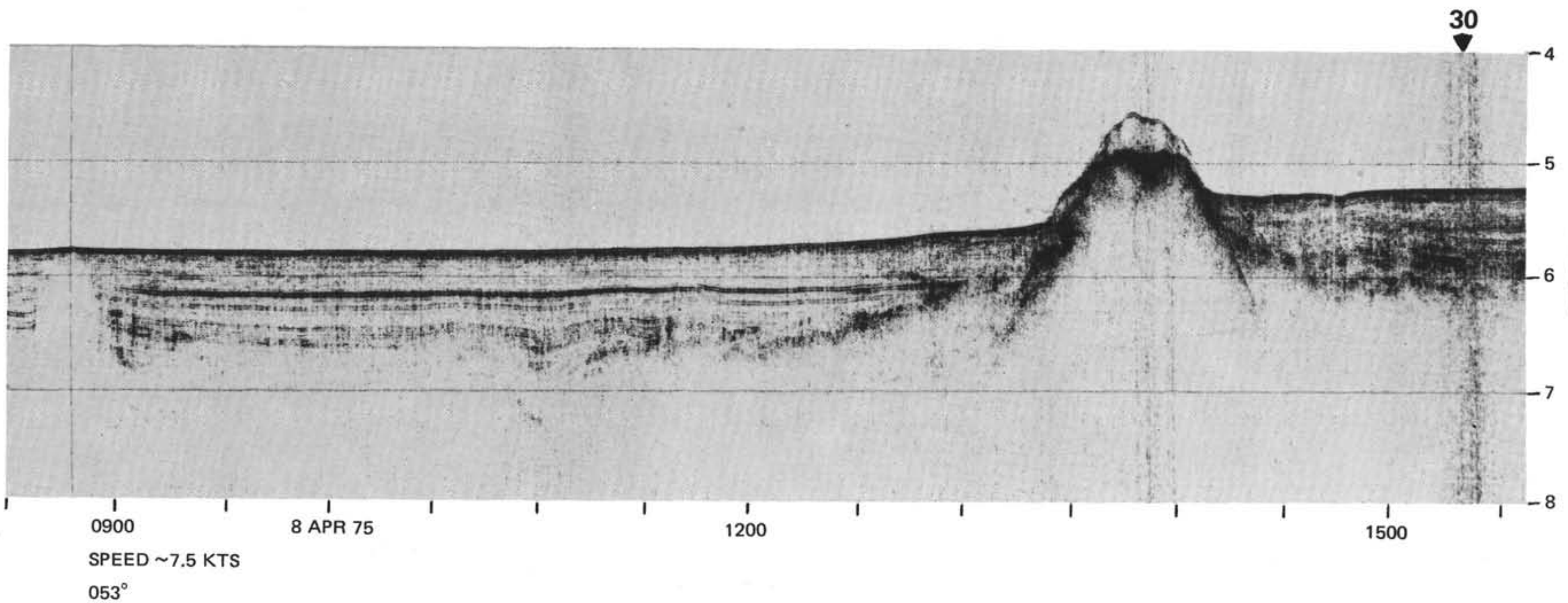

Figure 37. *Seismic profiles along the track of* Glomar Challenger.

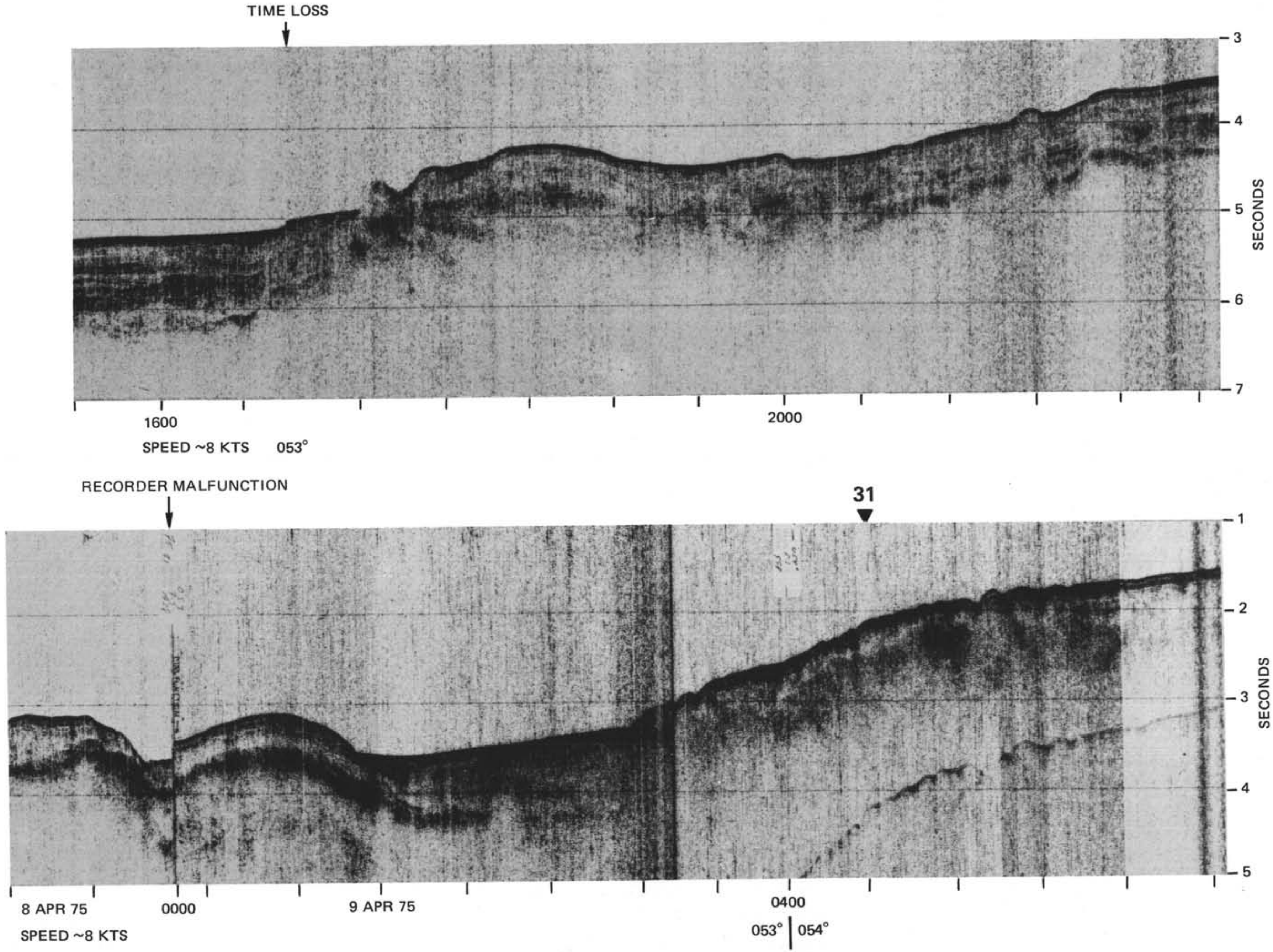

Figure 38. *Seismic profiles along the track of* Glomar Challenger.

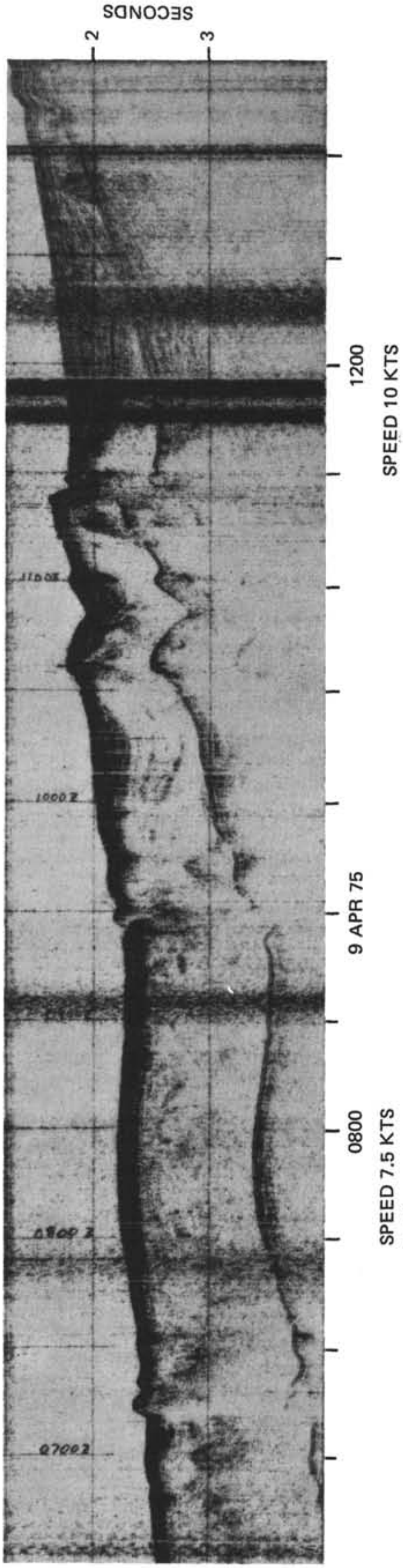

Figure 39. *Seismic profiles along the track of* Glomar Challenger.

SEISMIC REFLECTION PROFILES

The first part of the track, from Abidjan to the Sierra Leone Rise runs along the African continental margin in the northwestern part of the Gulf of Guinea where numerous canyons are cut at approximately right angles. Some of these canyons show clearly a sedimentary fill. A broad bathymetric high observed between 2100 hr on 18 February and 0600 hr on 19 February probably corresponds with the landward extension of the Saint-Paul Fracture Zone. Slightly thereafter the track cut obliquely down through the Continental Slope off Liberia and a set of parallel reflectors becomes apparent. They gently slope toward the abyssal plain while remaining roughly parallel to the sea floor. The uppermost part of the sedimentary section shows features closely resembling the lower continental rise hills of the North American Atlantic Margin. Near the junction of the Continental Rise with the abyssal plain (around 1800 hr on 20 February) the basement becomes visible beneath two major reflectors. These reflectors remain clearly visible beneath the absssal plain although they are not always well defined and correspond more with reflecting zones than sharp reflectors. Badly defined diapiric structures might occur just before reaching the base of Sierra Leone Rise (between 2000 hr and 2130 hr, 21 February, and between 0100 and 0230 hr, 22 February). They show close resemblance with structures described by Lancelot and Embley (in press) as mud diapirs. No direct correlation of the main reflectors has been attempted from this area to adjacent deep basins, although it appears probable that the relatively strong reflector located at approximately mid-section within the sedimentary layer could correspond with Horizon A.

The section observed on Sierra Leone Rise consists of a set of parallel reflectors that sometimes look quite similar to those observed previously on the Continental Rise. The lowermost of the reflectors does not seem to correspond with basement and is rather smooth. In several occasions it appears faulted (especially between 0530 and 0830 hr) but the faulting does not affect the overlying reflectors and would then be restricted to the early Tertiary (see Site 366 Chapter). Two relatively large seamounts mark the northern end of the Sierra Leone Rise. They are surrounded by a volcanic apron that appears clearly interstratified within the sediment layers (see Figure 19). In the same area bottom current activity left traces visible on the seismic profiles. Figure 19 (lower) shows evidence of sediment displacement:erosion or nondeposition at left, transport and accumulation at right.

The region of the transition to the Cape Verde Basin is where the *Glomar Challenger* seismic profile is generally of poor quality except in the vicinity of Site 370, where the speed of the ship was considerably reduced. In general the "acoustic stratigraphy" of the Cape Verde Basin shows the presence of a series of parallel reflectors. Basement is not visible on the *Glomar Challenger* profile, but is known from the results of Site 370 as well as from other seismic profiles to be relatively close to the base of the lowermost reflecting zone (see Site Chapter, this volume). That reflecting zone which is seen only around Site 370 on the *Glomar Challenger* profile, on which it regionally extends from about 1.0 to 1.3 seconds below the sea floor and rises slightly at Site 370 (Figure 20), has been correlated with the presence of Upper Jurassic to Lower Cretaceous limestones resting directly on oceanic basement. Higher in the section two reflectors are visible in most of the Cape Verde Basin. The lowermost of these corresponds with the top of the black shales at both Sites 367 and 368 (see Site Chapters) and therefore is probably the equivalent of Horizon A* observed in the North American Basin (Hollister, Ewing, et al., 1972). The uppermost one is apparently the equivalent of Horizon A and has been correlated with lower Tertiary porcellanite and chert in most of the North Atlantic. Very close to the sea floor reflector, and very often impossible to separate from it, appears a strong reflector which apparently results from the transition from sand-rich Pliocene turbidites to overlying Quaternary marls.

To the north of the Cape Verde Basin the *Glomar Challenger* track leads into the large Cape Verde Island volcanic complex which is surrounded by a volcanic apron comparable to the one observed around the seamounts previously described. After a brief stop at Sal Island (Cape Verde Islands) the ship headed toward the north-east across the Cape Verde Rise which, on the profiles, is characterized by parallel and finely stratified reflectors. In the lower parts of the profile a sharp and discontinuous reflector was found to correlate with diabase sills at Site 368. Because these sills are found in the uppermost part of the black shales, they produce reflectors that appear almost in continuity with the reflector that characterizes the top of that sedimentary unit.

Toward the north-east a transition is observed from the Cape Verde Rise to the Continental Rise off Mauretania. The acoustic character of the section changes gradually and reflectors become more diffuse and discontinuous. This acoustic character might be related to the presence of deep-sea fan type of sedimentation in that part of the Continental Rise. Further north the profile intersects the Continental Slope, characterized by abundant canyon with clearly displayed erosional features. Site 369 is located on the Continental Slope, off Spanish Sahara. After departing Site 369 the *Glomar Challenger* track runs along the volcanic edifices of Fuerteventura and Lanzarote (Canary Islands). The profile suggests a thick accumulation of finely stratified sediments (probably turbidites) on the flanks of these volcanic piles. The large flat-topped elevation observed on the profile, about 50 miles north of the islands, represents an oblique cross section of the submarine northern extension of the Fuerteventura-Lanzarote structural trend.

Just north of this structural high the ship track enters the Moroccan Basin which is characterized by relatively thick sediment accumulations. At first the section appears typical of a continental rise with finely stratified parallel reflectors, and the sea floor is seen to deepen gradually toward the north. At about 1030 hr on 28 March 1975 the track crosses the Agadir Canyon. The cross section of this valley is assymetrical, with the northern flank (corresponding to the right-hand side of turbidity currents flowing down the canyon) being higher and characterized by an internal structure closely resembling a "levee." In the deep part of the basin, where Site 370 was drilled, the profile is of very poor quality and does not allow for a discussion of the different reflectors present in the area (see Site Chapter for more details). Shortly after leaving Site 370, the track runs over several diapiric structures (generally believed to correspond with Jurassic to Triassic evaporites) piercing through the layered sediments of the Seine Abyssal Plain. Then the profile runs along the lower continental slope off northwest Morocco, and crosses obliquely the lower portion of the Rabat Canyon (around 0130 to 0230 hr on 9 April 1975) which marks the limit between the North African Continental Margin and a sediment accumulation believed to correspond with the seaward extension of the Miocene "nappes" of the Rif region in Northern Morocco. The record was terminated shortly before entering the Straits of Gibraltar to allow for more flexibility in the maneuvering of the vessel in that dense traffic area.

REFERENCES

Hayes, D.E. and Rabinowitz, P.D., 1975. Mesozoic magnetic lineations and the magnetic quiet zone off northwest Africa: Earth. Planet. Sci. Lett., v. 28, p. 105-115.

Hollister, C.D., Ewing, J.I., et al., 1972. Initial Reports of the Deep Sea Drilling Project, Volume 11: Washington (U.S. Government Printing Office).

Lancelot, Y. and Embley, R.W., in press. Evidence for widespread occurrence of sediment diapirism in the Deep Sea: Am. Assoc. Petrol. Geol. Bull.

Talwani, M., 1969. A computer system for the reduction, storage, and display of underway data acquired at sea: Lamont-Doherty Geol. Obs. Columbia Univ. Tech. Rept. 1, CU-1-69 N00014-67-A-0108-0004.

Talwani, M., Dorman, J., Worzel, J.L., and Bryan, G.M., 1966. Navigation at sea by satellite: J. Geophys. Res., v. 71, p. 5891-5902.